JOC The Journal of Organic Chemistry

Article

pubs.acs.org/joc

Design, Synthesis, and Evaluation of Inhibitors of Pyruvate Phosphate Dikinase

Chun Wu, Debra Dunaway-Mariano, and Patrick S. Mariano*

Department of Chemistry and Chemical Biology, University of New Mexico, Albuquerque, New Mexico 87131, United States

Supporting Information

ABSTRACT: Pyruvate phosphate dikinase (PPDK) catalyzes the phosphorylation reaction of pyruvate that forms phosphoenolpyruvate (PEP) via two partial reactions: PPDK + ATP + P_i → PPDK-P + AMP + PP_i and PPDK-P + pyruvate → PEP + PPDK. Based on its role in the metabolism of microbial human pathogens, PPDK is a potential drug target. A screen of substances that bind to the PPDK ATP-grasp domain active site revealed that flavone analogues are potent inhibitors of the *Clostridium symbiosum* PPDK. In silico modeling studies suggested that placement of a 3−6 carbon-tethered ammonium substituent at the 3′- or 4′-positions of 5,7-dihydroxyflavones would result in favorable electrostatic interactions with the PPDK Mg-ATP binding site. As a result, polymethylene-tethered amine derivatives of 5,7-dihydroxyflavones were prepared. Steady-state kinetic analysis of these substances demonstrates that the 4′-aminohexyl-5,7-dyhydroxyflavone **10** is a potent competitive PPDK inhibitor (K_i = 1.6 ± 0.1 μM). Single turnover experiments were conducted using 4′-aminopropyl-5,7-dihydroxyflavone **7** to show that this flavone specifically targets the ATP binding site and inhibits catalysis of only the PPDK + ATP + P_i → PPDK-P + AMP PP_i partial reaction. Finally, the 4′-aminopbutyl-5,7-dihydroxyflavone **8** displays selectivity for inhibition of PPDK versus other enzymes that utilize ATP and NAD.

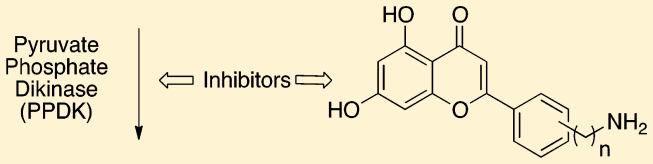

INTRODUCTION

Pyruvate phosphate dikinase (PPDK; EC 2.7.9.1) catalyzes the reversible phosphorylation reaction of pyruvate, adenosine 5′-triphosphate (ATP), and inorganic phosphate (P_i) that forms phosphoenolpyruvate (PEP), pyrophosphate (PP_i) and AMP.[1] PPDK is activated by divalent and monovalent metal ions. In vivo, Mg^{2+} and NH_4^+ serve as the cofactors.[2,3] The results from extensive studies[4−7] demonstrated that the chemical pathway of the *Clostridium symbiosum* PPDK catalyzed reaction, shown in Scheme 1, is initiated by nucleophilic substitution of the His455 imidazole N-3 nitrogen at the β-phosphorus of ATP to yield AMP and a pyrophosphorylated enzyme intermediate (PPDK-PP). This step is followed by P_i attack at the terminal phosphoryl group of the PPDK-PP to form PP_i and the phosphorylated histidine enzyme intermediate PPDK-P, which then participates in phosphorylation of pyruvate to form PEP.

Scheme 1

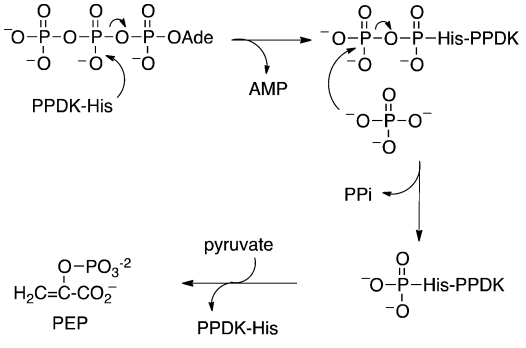

The PPDK monomer comprises three sequential functional domains (see Figure 1).[8−11] The N-terminal domain has an ATP-Grasp fold[12] that forms an active site crevice where ATP, P_i ,and Mg^{2+} bind. The C-terminal domain is an α,β-barrel, the N-terminal edge of which forms the subunit interface of the functional homodimer, with the C-terminal edge supporting an active site crevice where pyruvate and Mg^{2+} bind. The small globular α,β-fold central domain is connected to the terminal domains by helical peptide linkers. The catalytic His455 residue, which is located on the surface of this domain, transfers the phosphoryl group from donor to acceptor as the central domain alternates with a swivel-like motion between the active site of the N-terminal domain (conformer 1) and the active site of the C-terminal domain (conformer 2) (Figure 1).[11,13]

The biological range of PPDK is limited to specialized plants, protozoa, and bacteria.[14−23] Because of the small ΔG^o of its catalyzed reaction, PPDK can function in either direction and thus fill different functional niches.[1] PPDKs of plants[24] and photosynthetic bacteria (e.g., *Chlorobium tepidum*)[25] function in PEP production, a requirement for carbon dioxide fixation. In the typanosomatids, PPDK is located in the glycosomes where it functions in the recycling of pyrophosphate.[26] For the single cell protists and anaerobic bacteria, PPDK functions in a novel

Special Issue: Howard Zimmerman Memorial Issue

Received: September 2, 2012
Published: October 24, 2012

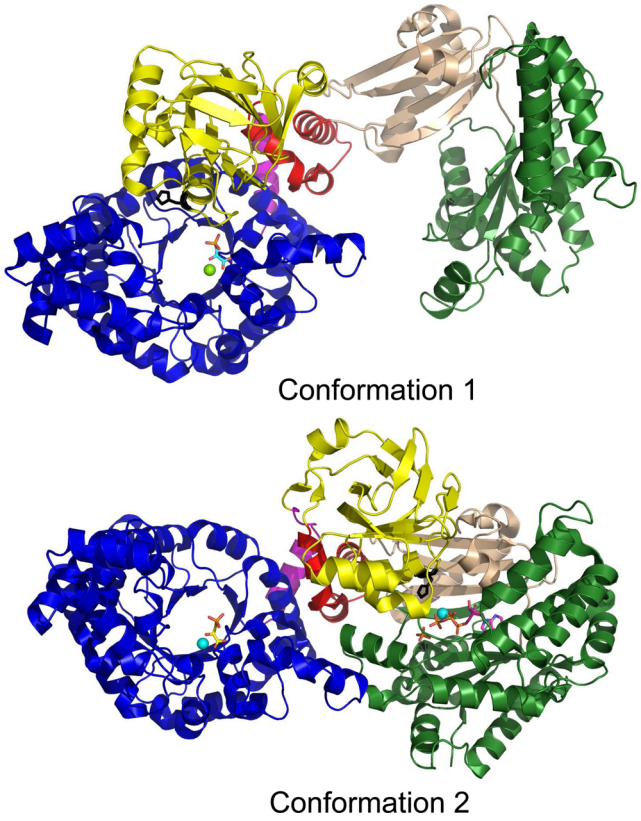

Figure 1. Pymol diagrams of the *Clostridium symbiosum* PPDK monomer in conformations 1 and 2. Catalysis of the ATP + P_i partial reaction takes place in the N-terminal domain (subdomains are colored forest green and wheat) active site in conformation 1, and catalysis of the PPDK-P + pyruvate partial reaction takes place in the C-terminal domain (colored blue) active site in conformation 2. Movement of the catalytic His455 residue (shown as black stick) between the two active sites is perceived to occur through interconversion of conformers 1 and 2 via swiveling of the central domain (colored yellow) about its helical linkers (colored red and magenta). The Mg^{2+} cofactors are shown as cyan spheres. The PEP is shown in stick form with carbon atoms colored yellow, nitrogen blue, oxygen red, and phosphorus orange. The P_i and ATP ligands are shown in stick form with the same color-coding except the carbon atoms, which are colored magenta.

pyrophosphate-dependent glycolytic pathway,[21,27,28] which is the key source of chemical energy because the proteins that support the citric acid cycle and oxidative phosphorylation are absent. The *Entamoeba histolytica* PPDK has been shown to exert significant control of glycolytic flux.[27] PPDK gene knockdown experiments carried out in *Giardia lamblia* have shown that the level of ATP is reduced to 3% of the normal level.[28] These organisms in particular are likely to be especially sensitive to inhibitors that block the function of PPDK.

PPDK has long been recognized as a logical target for herbicide development[29] because C4 plants, in which it is mainly found, are primary members of the "weed" family. PPDK is also present in the economically important bacterial plant pathogens of the genus *Phytophthora*, which are known to damage agricultural crops and to destroy natural ecosystems.[21] Moreover, the PPDK gene is found in numerous human bacterial pathogens including *Porphyromonas gingivalis, Treponema palladium, Rickettsia conorii, Clostridium tetani,* and *Streptococcus faecalis* and the protozoan human pathogens *Giardia, Entamoeba, Trichomonas, Leishmania,* and *Trypanosoma.* PPDK has also been found in the *Wolbachia* endosymbiont from the filarial parasite *Brugia malayi.*[16] Because it is not present in higher organisms, PPDK holds great potential as a target for the development of therapeutic agents to treat the infectious diseases caused by these pathogens. The goal of the effort described below was to identify a small molecule inhibitor that might serve as a lead in the development of such agents.

PPDK catalysis operates from two active sites, either of which could be targeted for inhibition. The active site that catalyzes the third partial reaction (PPDK-P + pyruvate ⇔ PPDK + PEP) is located at the top of the β-barrel and is largely comprised of polar residues. Oxalate, a mimic of the pyruvate enolate anion intermediate, is a powerful PPDK inhibitor;[10] however, this substance is not a promising lead for inhibitor design. Instead, our attention focused on the N-terminal domain active site where catalysis of the first two partial reactions (PPDK + ATP + P_i ⇔ PPDK-PP + AMP + P_i ⇔ PPDK-P + AMP + PP_i) occurs. As shown in Figure 2A, this domain contains a large cleft that is formed by the association of two subdomains. The snapshot of conformer 2 shown in Figure 1 indicates that the two subdomains dissociate, thereby expanding the cleft to facilitate substrate and Mg^{2+} cofactor binding, and then reassociate to close the active site for catalysis (conformer 1; Figures 1 and 2A).

As has been demonstrated with other ATP-dependent enzymes, the potential exists for inhibiting catalysis by using a tight-binding, space-filling ligand that blocks ATP binding.[30] The goal is to combine the binding energy derived from desolvation of matched nonpolar regions of the ligand and binding site with the binding energy and specificity derived from favorable electrostatic interaction between matched ligand and binding site polar substituents. In general, larger ligands provide a higher interaction potential than do smaller ligands, and thus, a "space-filling" ligand is desirable.

Inhibitor targeting of the ATP binding site of ATP-grasp enzymes is a relatively new endeavor.[31] Because the architecture of the ATP site of the ATP-grasp domain is so similar to that found in eukaryotic protein kinases, a logical starting point for inhibitor discovery would be screening of chemical libraries originally used for protein kinase inhibitor discovery. In this manner, a group from Pfizer identified several tight binding inhibitors belonging to the pyridopyrimidine structural class, which specifically target the ATP-grasp domain enzyme biotin carboxylase.[32] X-ray structural analyses of the enzyme−inhibitor complexes showed that the inhibitors bind to the ATP binding site where their respective phenyl substituents engage in hydrophobic interactions with the hydrophobic ribose binding region and the corresponding pyridopyrimidine unit engages in numerous hydrogen bond interactions with polar residues located in the adenine binding region.[32]

PPDK has been long recognized as a potential herbicide[29] and drug target[33] investigations aimed at inhibitor development have been limited to screenings of marine fungi and marine sponge derived extracts for inhibition of plant-derived PPDK.[34−36] Notably, the hydroxyquinones, ilimaquinone, ethylsmenoquinone, and smenoquinone, were reported to have inhibition constants in the high micromolar range. However, because these compounds show mixed-type inhibition vs ATP it is not clear at which site in the enzyme they are binding. On the other hand, the results from an in silico based screen of small molecule libraries against a *C. symbiosum* PPDK-derived homology model of the *Entamoeba histolytica PPDK*

dx.doi.org/10.1021/jo3018473 | J. Org. Chem. 2013, 78, 1910−1922

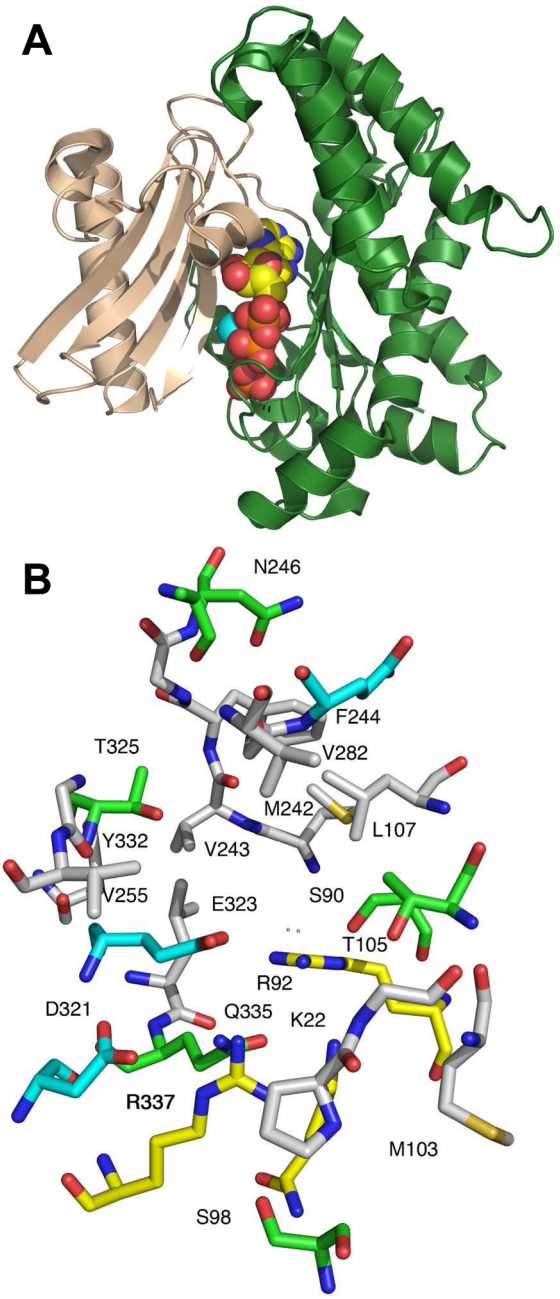

Figure 2. Pymol diagrams of the *Clostridium symbiosum* PPDK. (A) N-terminal domain with one subdomain colored wheat and the other forest green. The ATP (carbon is yellow, oxygen red, nitrogen blue, and phosphorus orange) atoms and Mg^{2+} ion (cyan) are shown as spheres. (B) The amino acid residues (shown in stick) that form the N-terminal domain active site. The carbon atoms of the nonpolar amino acids are colored white, those of the polar uncharged green, those of the negatively charged cyan and those of the positively charged yellow. All oxygen atoms are red, all nitrogen atoms blue, and all sulfur atoms yellow.

suggest that the ATP binding site is a good candidate for inhibition by a large space-filling ligand.[37]

Indeed, inspection of *C. symbiosum* PPDK N-terminal domain active site reveals that the pattern of amino acid side chains that project into this expansive binding site is ideal for inhibitor binding (Figure 2B). Specifically, a cluster of charged residues, which are available for favorable electrostatic interaction with an inhibitor, are located toward the front of the cleft. The rear of the binding site is lined with clusters of nonpolar residues, which could be paired with nonpolar segments of an inhibitor. Sprinkled throughout the cleft are individual uncharged, polar residues that can be targeted using hydrogen bond forming substituents of an inhibitor.

The PPDK encoding gene spread from bacteria to eukaryotes via lateral gene transfer and, consequently, the pairwise sequence identity between bacterial PPDK and eukaryotic PPDK is unusually high.[17] For instance, the sequence identity between *C. symbiosum* PPDK and *Entamoeba histolytica* is 52%, and notably the residues of the *C. symbiosum* PPDK N-terminal domain binding site pictured in Figure 2B are conserved. Furthermore, the X-ray structure of the PPDK from *Trypansoma brucei* PPDK[38] reveals that its ATP binding site is very similar to that in the bacterial enzyme. The *C. symbiosum* PPDK was utilized as a starting platform for the inhibitor discovery investigation because, in contrast to eukaryotic PPDKs, it is most amenable to biochemical and structural analysis. Here, we describe the results of studies that have led to the identification of flavone derivatives as selective, tight binding inhibitors of PPDK catalysis that act by competing with ATP for binding to the N-terminal domain active site.

RESULTS AND DISCUSSION

Discovery of a First-Generation PPDK Inhibitor. For the initial inhibitor screening effort, a large panel of compounds derived from several structural classes of protein kinase inhibitors,[39−41] including 3-substituted indolin-2-ones, purines, pyridopyrimidines, and flavonoids, were tested. In addition, the natural products balanol,[42] wortmannin,[43] and gossypol[44] were included in the screen. The previously described[4] spectrophotometric assay, based on the lactate dehydrogenase-NADH coupling reaction, was employed to monitor the initial velocities of the *C. symbiosum* PPDK-catalyzed reaction AMP + PP_i + PEP → ATP + P_i + pyruvate in the presence and absence of the inhibitor. The AMP concentration was set at 20 μM, which is twice the AMP K_m of 10 μM. Typically, owing to the limited water solubility, the maximum concentration of inhibitor that could be used in the experiment was restricted to 100 μM. In the event that no inhibition was observed, the smallest possible K_i value is reported to be greater than the inhibitor concentration. Given that 69 compounds were tested, structures and K_i values are reported in the Supporting Information (see Table SI1) rather than the text. Of the compounds screened, only two proved to be strong inhibitors. One of these, quercetin (**1**), is a member of the flavone natural product family, and the other is gossypol, a polyphenolic, binaphthyl disesquiterpene (**2**). Further kinetic analysis (Figure 3A,B) revealed that both compounds display competitive inhibition vs AMP with respective K_i values of 11.7 ± 0.5 and 15 ± 1 μM. The fact that competitive inhibition is observed is evidence that the inhibitors bind to the ATP binding site only.

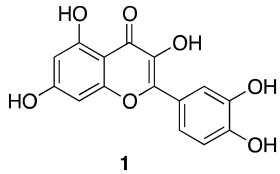

1

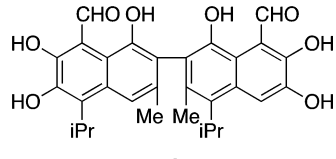

2

As a consequence of our expectation that the inhibitor development process would be more productive employing quercetin as a lead compound, a second screening that focused

dx.doi.org/10.1021/jo3018473 | J. Org. Chem. 2013, 78, 1910−1922

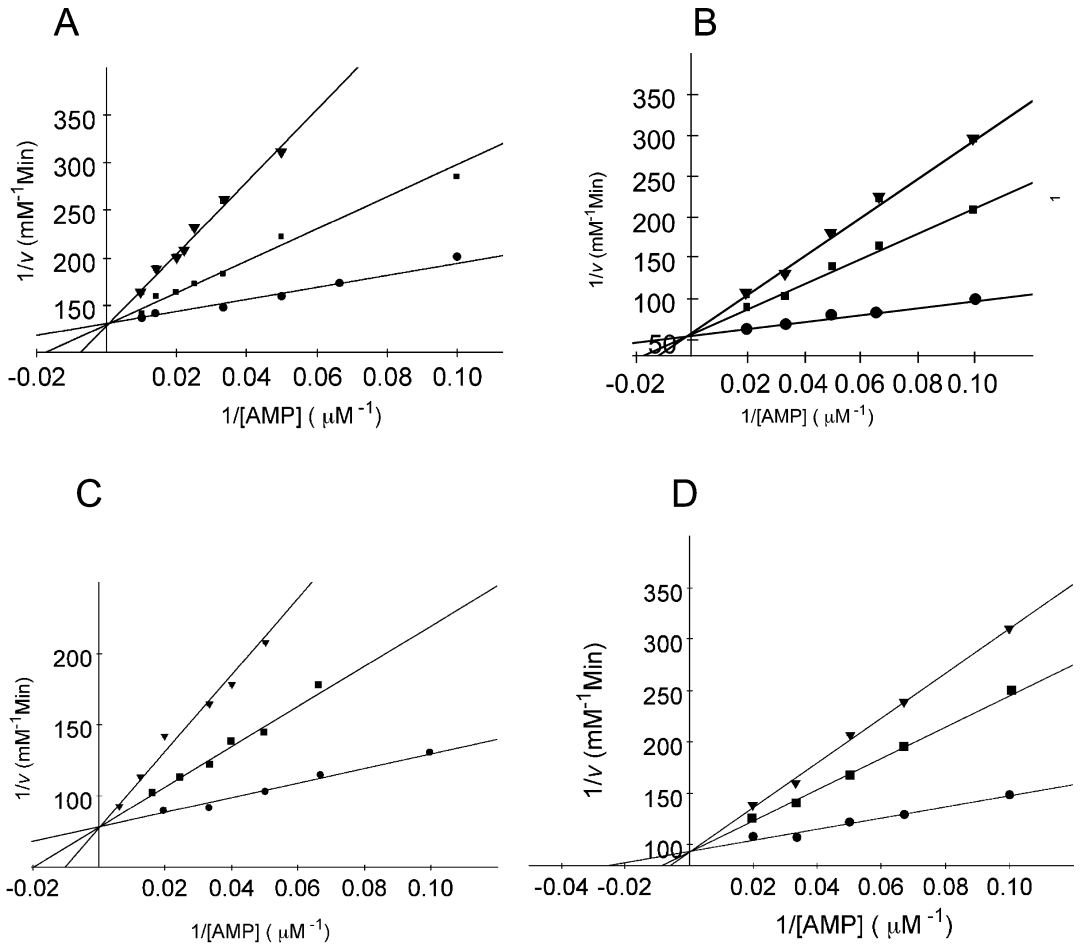

Figure 3. Double-reciprocal plot for the inhibition of PPDK by (A) 0(λ), 32.5(5), 50.0(τ) μM gossypol; (B) by 6.8 (λ), 14.8 (ν), 29.6(τ) μM) quercetin; (C) by 0(λ), 9.4(ν), 18.9 (τ) μM apigenin; (D) by 0(λ), 3.0 (ν), 4.5 (τ) μM aminoalkylflavone **10**. Assay solutions contained 5−80 μM AMP (range of 0.5- to 8-fold Km), 0.5 mM PEP, 1 mM PP_i, 5 mM $MgCl_2$, 40 mM NH_4Cl, 0.2 mM NADH, 20 units/mL lactate dehydrogenase in 20 mM imidazole buffer at pH 6.8 and 25 °C.

on flavones was carried out (see Table 1). Twenty-four commercially available and two synthetic (flavone and quercetin-3,5,7,3′,4′-pentamethyl ether) flavones were tested as inhibitors using the single-point diagnostic test (at 57−100 μM, vide supra) to estimate the K_i values. In cases where no inhibition was observed, the minimal value of K_i possible is reported to be greater than the concentration of inhibitor used in the assay. Flavones that do display significant inhibition were subjected to full kinetic analysis to demonstrate competitive inhibition vs AMP and to determine the inhibition constant. The results are reported in Table 1.

An analysis of the inhibition data displayed in Table 1 reveals factors that govern binding of flavones to the ATP-grasp site of PPDK. First, it appears that substances containing isoflavone-type structures, such genistein (**4**) and daidzin (**5**), have low PPDK binding affinities. Second, (±)-taxifolin (**6**), a flavonol which is otherwise identical to quercetin except for the absence of a 2,3-double bond, binds 3-fold less tightly to the ATP-site of the enzyme than does quercetin. Thus, the presence of double bond in the flavone B-ring is moderately important for inhibitory activity. Third, flavones that possess either no or one phenolic hydroxyl group are also poor PPDK inhibitors (e.g., flavone and quercetin-3,5,7,3′,4′-pentamethyl ether). In contrast, when at least two hydroxyl groups are present on the flavone skeleton, dramatic improvements in inhibitory activities take place. Among the group of flavones containing three hydroxyl groups, apigenin displays the highest PPDK inhibitory activity (K_i = 6 μM) (Figure 3C). Importantly, removal of the C-5 and C-7 hydroxyl groups (e.g., 4′-hydroxyflavone, K_i > 68 μM) results in a decrease in binding to PPDK. However, removal of the C-4′ hydroxyl group (e.g., 5,7-dihydroxyflavone K_i = 16 μM) causes only a small decrease in binding affinity. Furthermore, the presence of bulky polar groups, such as an *o*-rhamnoside, in place of a hydroxyl hydrogen leads to greatly reduced inhibition (quercetin, K_i = 11.7 μM, vs quercetrin, K_i >100 μM). Finally, flavones containing five hydroxyl groups have similar inhibitory activities as those with four hydroxyl groups as long as two are located at the C-5 and C-7 positions.

Second-Generation Inhibitor Design and Docking Studies. Comparison of the structures of the Src family tyrosine kinase Hck bound with AMPPNP vs bound with quercetin reveals that quercetin binds in the same position as does the AMPPNP adenine ring. The adenine binding site in PPDK combines nonpolar side chains that contribute to desolvation-driven binding with backbone amides that can potentially be engaged in hydrogen bonding with one or more of the flavone carbonyl/hydroxyl substituents. Notably, the remainder of the expansive active site is yet to be filled. Three residues Glu-323, Asp-321, and Gln-335, clustered on one side of the unfilled site, are believed to surround the magnesium ion

dx.doi.org/10.1021/jo3018473 | *J. Org. Chem.* 2013, 78, 1910−1922

Table 1. Flavone Competitive Inhibition Constants (K_i) or IC_{50} Values for PPDK[a]

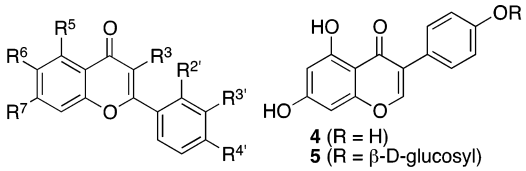

flavone	substituents R3	R5	R6	R7	R2′	R3′	R4′	solvent	[b,c] K_i (μM)
4, genistein								2% DMSO	>100[c]
5, daidzin								0.4% DMSO	>100[c]
6, (±)-taxifolin								H_2O	27 ± 1[b]
quercitrin	ORib	OH	H	OH	H	OH	OH	2% DMSO	>100[c]
quercetin pentamethyl ether	OMe	OMe	H	OMe	H	OMe	OMe	2% DMF	>100[c]
quercetin tetramethyl ether	OMe	OH	H	OMe	H	OMe	OMe	8%DMSO	>70[c]
acacetin	H	OH	H	OH	H	H	OMe	H_2O	>100[c]
dismetin	H	OH	H	OH	H	OH	OMe	2% DMSO	16.4 ± 0.2[b]
flavone	H	H	H	H	H	H	H	5% DMSO	>100[c]
3-hydroxyflavone	OH	H	H	H	H	H	H	4% DMSO	>75[c]
5-hydroxyflavone	H	OH	H	H	H	H	H	4% DMSO	>76[c]
7-hydroxyflavone	H	H	H	OH	H	H	H	H_2O	>57[a]
4′-hydroxyflavone	H	H	H	H	H	H	OH	H_2O	>68[c]
5,4′-dihydroxyflavone	H	OH	H	H	H	H	OH	H_2O	18 ± 1[c]
5,7-dihydroxyflavone	H	OH	H	OH	H	H	H	H_2O	16 ± 1[b]
7,2′-dihydroxyflavone	H	H	H	OH	OH	H	H	H_2O	15 ± 1[b]
7,3′-dihydroxyflavone	H	H	H	OH	H	OH	H	H_2O	22 ± 4[b]
apigenin	H	OH	H	OH	H	H	OH	H_2O	5.9 ± 0.1[b]
3,3′,4′-trihydroxyflavone	OH	H	H	H	H	OH	OH	H_2O	15 ± 1[b]
baicalein	H	OH	OH	OH	H	H	H	2% DMSO	21.9 ± 0.2[b]
5,7,2′-trihydroxyflavone	H	OH	H	OH	OH	H	H	H_2O	13 ± 1[b]
lueolin	H	OH	H	OH	OH	OH	H	H_2O	14 ± 1[b]
fisetin	H	OH	H	OH	H	OH	OH	H_2O	13.4 ± 0.5[b]
kaempferol	OH	OH	H	OH	H	H	OH	H_2O	8.8 ± 0.7[b]
quercetin	OH	OH	H	OH	H	OH	OH	H_2O	11.7 ± 0.5[b]
morin	OH	OH	H	OH	OH	H	OH	H_2O	9.1 ± 0.4[b]

[a]The 1 mL assay solutions initially contained 5−80 μM AMP (K_i determination) or 20 μM AMP (IC_{50} determination), 0.5 mM PEP, 1 mM PP_i, 5 mM $MgCl_2$, 40 mM NH_4Cl, 0.2 mM NADH, 20 units/mL lactate dehydrogenase in 20 mM imidazole buffer (pH 6.8). [b]Determined using a full kinetic analysis to demonstrate competitive inhibition vs AMP. [c]Estimated using a single-point diagnostic test (at 57−100 mM, vide supra) and a minimal value is reported to be greater than the concentration of inhibitor used in the assay.

of the bound magnesium−ATP complex. By tethering an alkyl ammonium group to the phenyl ring of 5,7-dihydroxyflavone we hoped to target the amino acid triad through favorable electrostatic interactions. In order to test this proposal, several dihydroxyflavones (**7**−**12**) with structures that contain amino-terminated alkyl substituents attached to the C-ring were designed, prepared, and evaluated as second-generation PPDK inhibitors. A selected member of this series, 4′-aminopropyl-5,7-dihydroxyflavone **7**, was first subjected to docking studies to determine if it might bind to the active site in an orientation that places the flavone moiety in the adenine binding site and the ammonium group juxtaposed to the side chains of the side chains of Glu-323, Asp-321, and Gln-335. Inspection of the lowest energy conformer, shown superimposed on ATP in the PPDK complexes in Figure 4, reveals that the surface the of 5,7-dihydroxyflavone ring in **7** overlaps nearly completely with that of the ATP adenine ring. Furthermore, the terminal ammonium ion is well positioned to interact with the PPDK Glu 323, Asp 321, and Gln 335 side chains.

Encouraged by the results from the docking exercise, we undertook the synthesis of the aminopropyl-5,7-dihydroxyflavone **7** as well as analogues in which the length of the alkyl linker is longer (**8**−**10**) for testing as PPDK inhibitors. The aminoalkyldihydroxyflavone **11** was also prepared to evaluate the affect of repositioning the linker, whereas **12** was prepared to test the impact of the restriction of conformational motion in the alkyl linker. The synthetic sequences employed for the preparation of **7**−**12** are shown in Schemes 2 and 3.

The aminoalkylflavones **7**−**12** were evaluated as competitive inhibitors vs AMP, and the inhibition constants obtained are displayed in Table 2. The results of this kinetic analysis clearly show that incorporation of 3−6 carbon-containing, ammonium ion terminated chains at the 4′-position of the 5,7-dihydroxyflavone ring system results in a decrease in K_i, which in the best inhibitor has been reduced by an order of magnitude. In addition, placement of a 6-carbon-tethered ammonium substituent at the 3′-position of 5,7-dihydroxyflavone (as in **11**) results in the same degree of improvement in PPDK binding as is seen in the 4-linked analogs. Finally, the observation that the amino-*trans*-butenyl-flavone **12** binds 10-fold less tightly than its saturated four-carbon analogue **8** suggests that side chain flexibility is an important factor governing binding.

dx.doi.org/10.1021/jo3018473 | J. Org. Chem. 2013, 78, 1910−1922

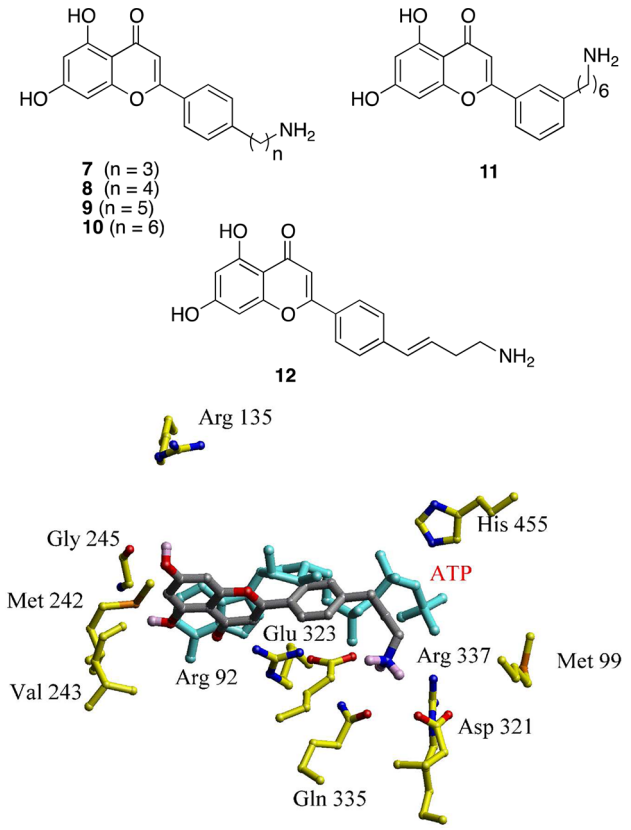

Figure 4. Overlays of docked structures of the PPDK complexes with aminopropylflavone **7** (carbon, gray; nitrogen, blue; oxygen, red; hydrogen, pink) and ATP (cyan). PPDK residues are colored as follows: nitrogen, blue; oxygen, red; sulfur, orange; carbon, yellow. Some residues are removed for clarity.

Aminoflavone 7 Targets the PPDK ATP Site. To demonstrate that PPDK inhibition by the aminoalkyldihydroxyflavones derives solely from binding to the N-terminal domain active site, we employed transient kinetic techniques to separately test the inhibition of a single turnover reaction catalyzed at the N-terminal domain active and the inhibition of a single turnover reaction catalyzed at the C-terminal domain active. Accordingly, the time course for the single turnover reaction, PPDK + [^{14}C]ATP + P_i → PPDK-P + [^{14}C]AMP + PP_i, catalyzed by the enzyme in the presence and absence of the representative aminoalkyldihydroxyflavone **7** is shown in Figure 5. The K_i = 3.3 μM derived from these data closely match the K_i = 2.8 μM (Table 2) determined using steady-state kinetic techniques.

Next, single time point (600 ms) measurements (percent conversions) were made for the single turnover reaction, PPDK + [^{14}C]PEP → PPDK-P + [^{14}C]pyruvate, in the presence and absence of **7** (see Table 3). As the results show, even at a very high concentration (800 μM, from Table 2 the K_i measured for the steady-state reaction is 2.8 μM) of **7**, no inhibition takes place. Thus, studies of the two partial reactions clearly demonstrate that aminopropylflavone specifically targets the N-terminal domain active site.

Aminoalkylflavone (8) Enzyme Specificity. The final question that we addressed concerns whether the aminoalkyldihydroxyflavones discriminate between the ATP binding site in PPDK and the ATP binding sites in other ATP-dependent enzymes. Although the PPDK ATP binding site is located in an ATP-Grasp domain, it does not closely resemble ATP binding sites in other ATP-Grasp domains. This is a consequence of the fact that the ATP-Grasp domain is used to catalyze ligase reactions. Thus, as a kinase, PPDK is an outlier to the ATP-Grasp enzyme superfamily.[31] The ATP binding sites of protein kinases in general, and cAMP-dependent protein kinase in particular, most closely resemble that of PPDK. Therefore, we tested the inhibition of cAMP-dependent protein kinase by the representative aminoalkyldihydroxyflavone **8** and observed that it is a competitive inhibitor of this kinase vs ATP with a K_i = 15 μM (Table 4). Thus, this inhibitor binds to PPDK 8-fold more tightly than it does to cAMP-dependent protein kinase.

Next, we examined a variety of kinases that function in cellular metabolism. Of these, **8** served as an inhibitor of only pyruvate kinase, which like the other kinases possesses an ATP binding site that has no resemblance to that of PPDK. Nevertheless, the K_i = 34 μM value observed is still 20-fold greater than that observed for inhibition of PPDK by **8**. Finally, hexokinase, myokinase, and acetate kinase were not inhibited at 129 μM **8** nor was the NADH-dependent enzyme lactate dehydrogenase.

■ CONCLUSIONS

The results presented here demonstrate that 5,7-dihydroxyflavones possessing properly positioned aminoalkyl chains are potent inhibitors of PPDK and that they act through competitive binding at the enzyme's ATP binding site. The flavone unit is an effective replacement of the ATP adenine ring as shown by tight binding of apigenine. Placement of 3−6 carbon-tethered ammonium substituents at the 3′- or 4′-positions of the 5,7-dihydroxyflavone skeleton results in tighter binding which we propose is the result of favorable electrostatic interactions between the positively ammonium ion and one or more of the residues that form the triad Glu323, Asp321, and Gln-335, otherwise positioned to interact with the ATP bound Mg^{2+}.

The results of steady-state kinetic analysis demonstrate that, in the series of substances explored, 4′-aminohexylflavone **10** (K_i = 1.6 ± 0.1 μM) is the most potent competitive PPDK inhibitor vs AMP. To confirm that the second-generation flavones specifically target the ATP binding site, single turnover experiments were conducted using aminopropylflavone **7** to demonstrate that this substance inhibits catalysis of the PPDK + ATP + Pi → PPDK-P + AMP partial reaction and not the ensuing PPDK-P + pyruvate → PEP + PPDK partial reaction. Finally, the second-generation 4′-aminobutyl-flavone **8** was observed to display selectivity for inhibition of PPDK versus other enzymes that utilize ATP as a substrate.

■ EXPERIMENTAL SECTION

General Methods. All reactions were run under a nitrogen atmosphere. Unless otherwise noted, all reagents were obtained from commercial sources and used without further purification. ^{1}H and ^{13}C NMR spectra were recorded on $CDCl_3$ solutions unless otherwise specified, and chemical shifts are reported in ppm relative to residual $CHCl_3$ at 7.24 ppm (for ^{1}H NMR) and 77.0 ppm (for ^{13}C NMR). ^{13}C NMR resonance assignments were aided by the use of the DEPT technique to determine numbers of attached hydrogens. Mass spectra were recorded by using fast atomic bombardment (FAB) or electrospray (ES) techniques and a TOF instrument.

PPDK Purification and Assay. PPDK was purified from *Escherichia coli* JM 101 carrying the plasmid pACYC184-D12 as described previously.[45] The spectrophotometric assay, described

dx.doi.org/10.1021/jo3018473 | J. Org. Chem. 2013, 78, 1910−1922

Scheme 2

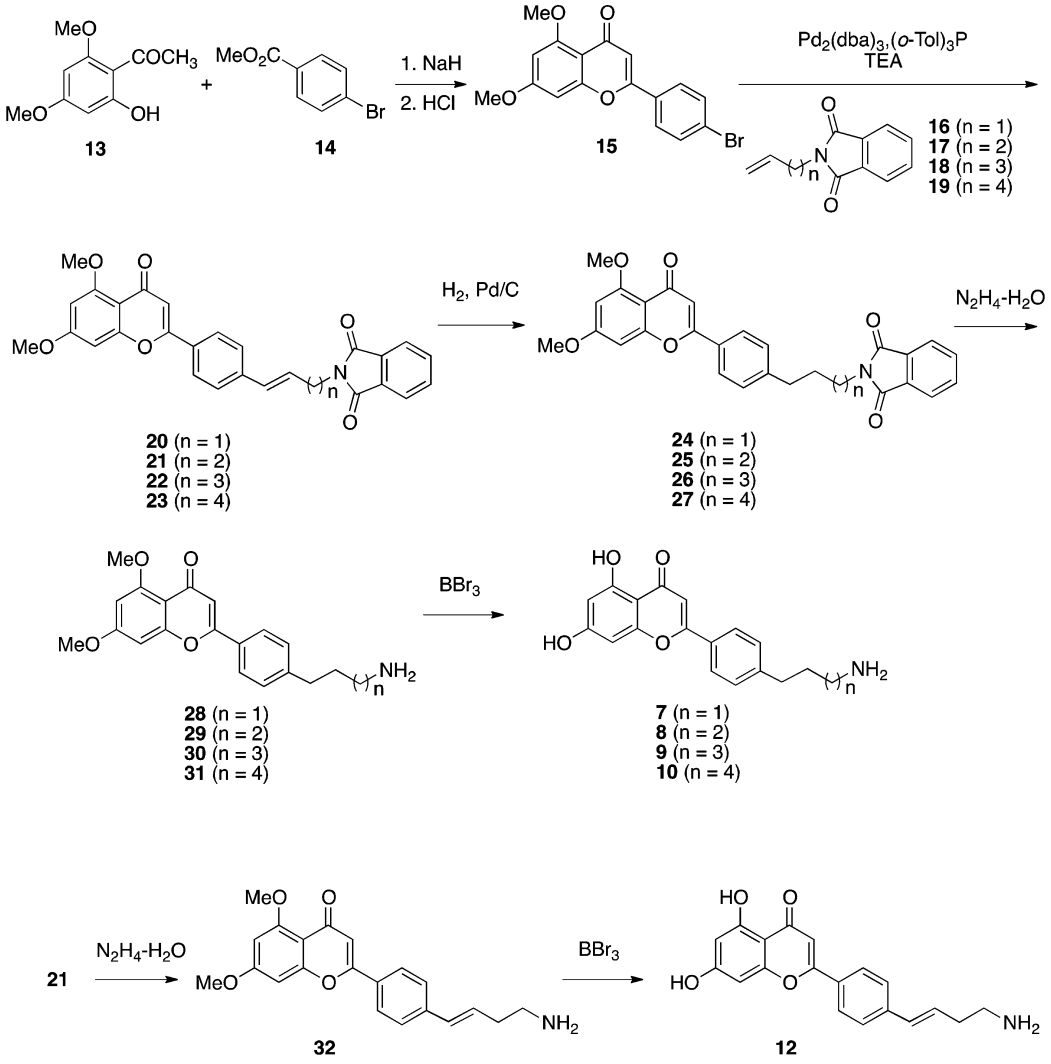

Scheme 3

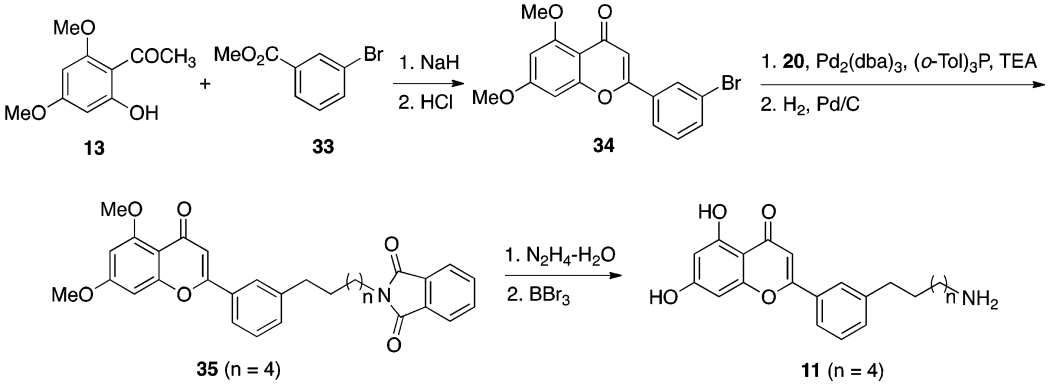

previously,[4] was used to monitor the initial velocity of PPDK-catalyzed reaction of AMP, PP_i, and PEP to ATP, P_i, and pyruvate. The overall reaction was monitored in the reverse direction (pyruvate formation) at 340 nm by using the lactate dehydrogenase (20 units/mL)−NADH (0.2 mM) coupling reaction. The initial velocity (v_0) data were analyzed using eq 1 and the computer programs described by Cleland.[46] The k_{cat} was calculated using eq 2

$$v_0 = v_{max}[E][S]/(K_m + [S]) \quad (1)$$

$$k_{cat} = v_{max}/[E] \quad (2)$$

where v_0 is the initial velocity, v_{max} is the maximum velocity, [E] is the enzyme concentration, [S] is the substrate concentration, and K_m is the Michaelis constant. The inhibition constants (K_i) for the inhibitors were determined from initial velocity data obtained at varying AMP concentrations and fixed, saturating concentrations of cosubstrates and cofactors. The initial velocity data were analyzed using eq 3, where K_i is the inhibition constant and [I] is the inhibitor concentration.

dx.doi.org/10.1021/jo3018473 | J. Org. Chem. 2013, 78, 1910−1922

Table 2. PPDK Inhibition Constants of Aminoalkylflavones[a]

flavone	K_i (μM)	flavone	K_i (μM)
10	1.6 ± 0.1		
7	2.8 ± 0.1	**11**	2.7 ± 0.4
8	1.8 ± 0.3	**12**	18.3 ± 0.1
9	2.6 ± 0.5	5,7-dihydroxyflavone	16 ± 2

[a]The 1 mL assay solutions initially contained 5−80 μM AMP, 0.5 mM PEP, 1 mM PP_i, 5 mM $MgCl_2$, 40 mM NH_4Cl, 0.2 mM NADH, 20 units/mL of lactate dehydrogenase in 20 mM imidazole buffer (pH 6.8).

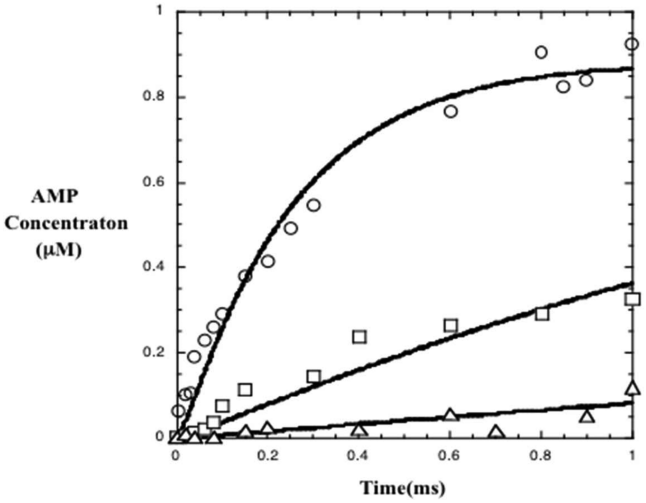

Figure 5. Time courses for [^{14}C]AMP formation in single turnover PPDK (7.2 μM) catalyzed reactions of 1.8 μM [^{14}C]ATP, 11 mM P_i, 5 mM $MgCl_2$, and 40 mM NH_4Cl in 50 mM K^+HEPES (pH 7.0, 25 °C) in the presence of 0 μM (○), 75 μM (□), and 150 μM (Δ) of the aminoalkylflavone **7**. The solid lines were generated by time course simulation using the simulation program KinSimand, the known kinetic model of which included the microscopic rate constants governing the steps of ATP + P_i + pyruvate partial reaction[7] and the dissociation constant governing the binding of the inhibitor to the free enzyme.

Table 3. Percent Conversions at 600 ms in the Single Turnover Reaction of PPDK + [^{14}C]PEP → PPDK-P + [^{14}C]Pyruvate Using 8 μM PPDK, 2 μM [^{14}C]PEP, 5 mM $MgCl_2$, and 40 mM NH_4Cl in 50 mM K^+HEPES (pH 7.0, 25 °C) along with 0, 82, and 800 μM of 7

concentration of 7 (μM)	conversion (%)
0	63
82	67
800	64

Table 4. Inhibition Constants of Aminobutylflavone 8 toward Lactate Dehydrogenase and Members of the Protein Kinase Family

enzyme	K_i (μM)	$K_{i(enzyme)}/K_{i(PPDK)}$
PPDK	1.8 ± 0.3	1
lactate dehydrogenase	>129	>72
hexokinase	>129	>72
myokinase	>129	>72
acetate kinase	>129	>72
pyruvate kinase	61 ± 7	34
cAMP dependent protein kinase	15 ± 3	8

$$v_0 = v_{max}[E][S]/[K_m(1 + [I]/K_i) + [S]] \quad (3)$$

For initial inhibitor screening, single-point diagnostic testing was carried out on 1 mL assay solution containing 20 μM substrate AMP (considering both the K_m of PPDK (ca. 10 μM) and the lowest detection limits of the UV spectrometer) and saturating concentrations of cosubstrates (0.5 mM PEP, 1 mM PP_i) and metal ion cofactors (5 mM $MgCl_2$ and 40 mM NH_4Cl) in 20 mM imidazole (pH 6.8, 25 °C) as described previously.[47] The concentrations of inhibitors tested in the 1 mL assay solution are 50 or 100 μM depending on compound availability. In each case, the reaction was initiated by the addition of PPDK.

When a compound showed obvious inhibitory activity (<40 μM), a more accurate assay was carried out in the manner as described below for quercetin. A quercetin stock solution was prepared (50 mg in 1 mL of 1 N NaOH). The stock solution was diluted 100-fold by H_2O addition to reach a concentration of 1.5 mM with a pH of 8. Aliquots (0, 10, and 20 μL aliquots of the 1.5 mM) of the stock inhibitor solution were added to 1 mL assay solutions containing 5−80 μM AMP, 0.5 mM PEP, 1 mM PP_i, 5 mM $MgCl_2$, 40 mM NH_4Cl, 0.2 mM NADH, and 20 units/mL of lactate dehydrogenase in 20 mM imidazole buffer (pH 6.8). In each case, the reaction was initiated by the addition of 0.012 μM PPDK. The initial velocities of reactions were measured as a function of AMP concentration in the absence and the presence of 5,7-dihydroxy-4′-[3-aminoprop-1-yl]flavone **7** (0, 6.4, 9.6, and 12.8 μM), 5,7-dihydroxy-4′-(3-aminobut-1-yl)flavone **8** (0, 4.3, 8.6 μM), 5,7-dihydroxy-4′-(3-aminobut-1-en-1-yl)flavone **12** (0, 39, 58 μM), 5,7-dihydroxy-4′-(3-aminopent-1-yl)flavone **9** (0, 4.2, 6.3 μM), 5,7-dihydroxy-4′-(3-aminohex-1-yl)flavone **10** (0, 3.0, 4.5 μM), and 5,7-dihydroxy-3′-(3-aminohex-1-yl)flavone **11** (0, 5.8, 7.7 μM).

Evaluation of Kinase and Dehydrogenase Inhibition by 5,7-Dihydroxy-4′-aminobutylflavone 8. Hexokinase. The initial velocity of *Saccharomyces cerevisiae* hexokinase-catalyzed reaction of glucose and ATP to glucose-6-phosphate and ADP was measured using the NADP/lactate dehydrogenase coupling system. Reaction solutions contained K_m levels of glucose and ATP, 5 mM $MgCl_2$, 0.4 mM NADP, 2 units/mL glucose-6-phosphate dehydrogenase, 0.03 units/mL hexokinase, and 0 or 130 μM 5,7-dihydroxy-4′-aminobutylflavone in 50 mM K^+HEPES (pH 7.0, 25 °C). The overall reaction was monitored at 340 nm (ε = 6.2 mM^{-1} cm^{-1}).

Pyruvate Kinase. The initial velocity of rabbit muscle pyruvate kinase-catalyzed reaction of PEP and AMP to pyruvate and ATP was measured using the NADH/lactate dehydrogenase coupling system. Reaction solutions contained the K_m level of PEP, 0.5−10-fold K_m levels of ADP, 5 mM $MgCl_2$, 0.2 mM NADH, 20 unit/mL lactate dehydrogenase, 40 units/mL pyruvate kinase, and 0, 43, or 86 μM 5,7-dihydroxy-4′-aminobutylflavone in 50 mM K^+HEPES (pH 7.0, 25 °C). The overall reaction was monitored at 340 nm (ε = 6.2 mM^{-1} cm^{-1}).

Myokinase. The initial velocity of rabbit muscle myokinase-catalyzed reaction of ATP and AMP to 2 × ADP was measured using the pyruvate kinase/PEP-NADH/lactate dehydrogenase coupling system. Reaction solutions contained K_m levels of AMP and ATP, 5 mM $MgCl_2$, 0.2 mM NADH, 1 mM PEP, 20 units/mL lactate dehydrogenase, 0.1 unit/mL myokinase, and 0 or 130 μM 5,7-dihydroxy-4′-aminobutylflavone in 50 mM K^+HEPES (pH 7.0, 25 °C). The overall reaction was monitored at 340 nm (ε = 6.2 mM^{-1} cm^{-1}).

Acetate Kinase. The initial velocity of *E. coli* myokinase-catalyzed reaction of ATP and acetate to acetylphosphate and ADP was measured using the pyruvate kinase/PEP-NADH/lactate dehydrogenase coupling system. Reaction solutions contained K_m levels of acetate and ATP, 5 mM $MgCl_2$, 0.2 mM NADH, 1 mM PEP, 20 units/mL of lactate dehydrogenase, 0.1 unit/mL of acetate kinase, and 0 or 130 μM 5,7-dihydroxy-4′-aminobutylflavone in 50 mM K^+HEPES (pH 7.0, 25 °C). The overall reaction was monitored at 340 nm (ε = 6.2 mM^{-1} cm^{-1}).

Lactate Dehydrogenase. Reaction solutions contained 100 μM pyruvate, 200 μM NADH, 0.1 unit/mL lactate dehydrogenase, and 0 or 130 μM 5,7-dihydroxy-4′-aminobutylflavone in 50 mM K^+HEPES (pH 7.0, 25 °C). The overall reaction was monitored at 340 nm (ε = 6.2 mM^{-1} cm^{-1}).

dx.doi.org/10.1021/jo3018473 | J. Org. Chem. 2013, 78, 1910−1922

Rapid Quench Analysis of the PPDK-Catalyzed Single Turnover Reaction E + [^{14}C]ATP + P_i →E−P +[^{14}C]AMP + PP_i. Single-turnover reactions of 7.2 μM wild-type PPDK, 1.8 μM [^{14}C]ATP, 11 mM P_i, 5 mM $MgCl_2$, and 40 mM NH_4Cl in 50 mM K^+HEPES (pH 7.0, 25 °C) were carried out in the presence 0, 75, and 150 μM 5,7-dihydroxy-4′-aminopropylflavone (**7**) using a rapid quench device from KinTek Instruments. Reactions were initiated by mixing 32 μL of 14 μM wild-type PPDK, 0, 147, or 295 μM 5,7-dihydroxy-4′-aminopropylflavone (**7**), 9.7 mM $MgCl_2$, and 77.5 mM NH_4Cl in 50 mM K^+HEPES (pH 7.0, 25 °C) with 30 μL of 3.7 μM [^{14}C]ATP and 22.7 mM P_i in 50 mM K^+HEPES (pH 7.0, 25 °C) and then terminated at specified times with 182 μL of 0.6 M HCl. The protein was removed from the acid quenched samples by centrifugation through a 500 μL filter (cutoff molecular mass of 30 kDa) purchased from Pall Gelman, Inc. The unconsumed [^{14}C]ATP and [^{14}C]AMP product were separated by HPLC using a Beckman Ultrasphere C18 reversed-phase analytical column and 25 mM KH_2PO4, 2.5% triethylamine, and 5% methanol as the mobile phase. The fractions containing ATP and AMP were analyzed for ^{14}C content by liquid scintillation counting. The percent conversion was deduced from the ratio of unconsumed [^{14}C]ATP and [^{14}C]AMP product. The AMP concentration was calculated by multiplying the initial substrate concentration by the percent conversion. The time course data of AMP formation were fit to single exponential equation (eq 4) using the KaleidaGraph program to yield the rate constants from the single turnover reactions

$$[B]_t = [B]_\infty\{1 - \exp(k_{obs}t)\} \quad (4)$$

where $[B]_t$ is the product AMP concentration at time t, $[B]_\infty$ is the product AMP concentration at equilibrium, and k_{obs} is the observed rate constant for the reaction.

Rapid Quench Analysis of Competitive Inhibition by Flavones toward the Single Turnover Reaction E + [^{14}C]PEP → E−P +[^{14}C]Pyruvate Catalyzed by the Wild-Type PPDK. Single-turnover reactions of 8 μM wild-type PPDK, 2 μM [^{14}C]PEP, 5 mM $MgCl_2$, and 40 mM NH_4Cl in 50 mM K^+HEPES (pH 7.0, 25 °C) were carried in the presence 0, 82, and 800 μM 5,7-dihydroxy-4′-aminopropylflavone (**7**) using a rapid quench device from KinTek Instrument. Reactions were initiated by mixing 32 μL of 15.5 μM wild-type PPDK, 0, 0.16, or 1.5 mM 5,7-dihydroxy-4′-aminopropylflavone (**7**), 9.7 mM $MgCl_2$, and 77.5 mM NH_4Cl in 50 mM K^+HEPES (pH 7.0, 25 °C) with 30 μL of 4.0 μM [^{14}C]PEP and 22.7 mM P_i in 50 mM K^+HEPES (pH 7.0, 25 °C) and then terminated at 600 ms with 182 μL of 0.6 M HCl. The protein was removed from the acid-quenched samples by centrifugation through a 500-μL filter (cutoff molecular mass of 30 kDa) purchased from Pall Gelman, Inc. The unconsumed [^{14}C]PEP and product [^{14}C]pyruvate were separated by HPLC using a Beckman Ultrasil anon-exchange column and 0.3 M KH_2PO_4, 0.6 M HCl pH = 5.0 as the mobile phase. The fractions containing PEP and pyruvate were analyzed for ^{14}C radioactivity by liquid scintillation counting. The percent conversion was deduced from the ratio of unconsumed [^{14}C]PEP and [^{14}C]pyruvate product.

Synthetic Procedures. General Methods. ^{1}H NMR spectra were recorded using $CDCl_3$ solutions (unless otherwise noted) at 500 and 250 MHz, and ^{13}C NMR spectra were recorded at 62.9 MHz. Chemical shifts are reported in ppm relative to internal standards. Infrared spectral bands are recorded in cm^{-1}. High-resolution mass spectra were obtained by using electron-impact ionization or FAB. All reagents and solvents were purchased from commercial sources and used without further purification unless otherwise specified. 2,4-Dimethoxy-6-hydroxyacephenone **14**[48] and phthalimido alkenes **17**−**20**[49] were prepared by using known procedures. All reactions were carried out under a nitrogen atmosphere. Analytical TLC was performed on 250 μm silica gel plates. Flash chromatography was performed by using 200−400 mesh silica gel 60. All synthetic intermediates were isolated as oils unless otherwise noted and shown to be >90% pure by ^{1}H and/or ^{13}C NMR analysis. The target aminoalkyl-flavones used for biochemical analyses were purified by using HPLC (C_{18} reversed-phase, H_2O−MeOH gradient) and shown to be comprised of single substances (>95% purity).

Synthesis of Aminoalkylflavones 7−10 and 12 (Scheme 2). 5,7-Dimethoxy-4′-bromoflavone (15). To a solution of methyl 4-bromobenzoate (**13**) (9.80 g, 45.5 mmol) and NaH 1.20 g (95% dispersion, 50 mmol) in DMF (20 mL) at 0 °C was added to a solution of 2,4-dimethoxy-6-hydroxyacetophenone (**14**) (3.00 g, 15.2 mmol) in DMF (50 mL). The mixture was stirred at 25 °C for 12 h and poured onto ice. The pH of the resulting solution was adjusted to 10 by addition of 1 N HCl and extracted with CH_2Cl_2. The CH_2Cl_2 extracts were concentrated in vacuo giving a residue, which was dissolved in $CHCl_3$. The $CHCl_3$ solution was saturated with gaseous HCl, stirred for 4 h at 25 °C, made basic by the addition of aq Na_2CO_3, and extracted with CH_2Cl_2. The CH_2Cl_2 extracts were dried and concentrated in vacuo giving a solid which was crystallized from DMF to afford 2.90 g (53%) of 3,5-dimethoxy-4′-bromoflavone (**15**) as white needles: mp 198.6−199.4 °C; ^{1}H NMR 7.71 (d, 2H, J = 8.6 Hz), 7.61 (d, 2H, J = 8.6 Hz), 6.63 (s, 1H), 6.54 (d, 1H, J = 2.2 Hz), 6.37 (d, 1H, J = 2.2 Hz), 3.93 (d, 2H, J = 19.7 Hz); ^{13}C NMR 177.0, 164.0, 160.7, 159.2, 132.0, 130.2, 127.1, 125.6, 108.9, 96.1, 92.6, 56.2, 55.6; HRMS (FAB) m/z $(M)^+$ calcd for $C_{17}H_{12}O_4{}^{79}Br$ 359.9997, found 360.0011.

5,7-Dimethoxy-4′-[3-(*N*-phthalimido)prop-1-en-1-yl]flavone (20). A mixture of 5,7-dimethoxyl-4′-bromoflavone (**15**) (2.0 g, 5.5 mmol), *N*-allylphthalimide **16** (1.2 g, 6.0 mmol), P(*o*-tol)$_3$ (275 mg, 0.3 mmol), and $Pd_2(dba)_3$ (400 mg, 1.2 mmol) in 50 mL of triethylamine was stirred at 110 °C for 12 h, cooled to 25 °C, and concentrated in vacuo. A solution of the residue in CH_2Cl_2 and was washed with H_2O, dried, and concentrated in vacuo giving a residue that was subjected to flash chromatography (silica gel, EtOAc then EtOH) to give 1.3 g (50%) of 5,7-dimethoxy-4′-(3-*N*-phthalimido-1-propen-1-yl)flavone (**20**) as white needles: mp 238 °C dec; ^{1}H NMR 7.86 (m, 2H), 7.82 (m, 2H), 7.72 (m, 2H), 7.45 (m, 2H), 6.70 (m, 2H), 6.54 (s, 1H), 6.35 (m, 2H), 4.46 (d, 2H, J = 6.5 Hz), 3.91 (d, 6H, J = 20.9 Hz); ^{13}C NMR 177.4, 167.9, 164.0, 160.8, 160.1, 139.0, 134.0, 132.5, 130.6, 126.9, 126.0, 125.0, 123.3, 108.8, 95.1, 92.8, 55.4,55.7, 39.5; HRMS (FAB) m/z $(M + H)^+$ calcd for $C_{28}H_{22}O_6N$ 468.1447, found 468.1465.

5,7-Dimethoxy-4′-[3-(*N*-phthalimido)prop-1-yl]flavone (24). A mixture of 5,7-dimethoxy-4′-[3-*N*-(phthalimido)prop-1-en-1-yl]-flavone (**20**) (1.6 g, 34 mmol), 10% Pd/C (0.1 g) in 40 mL of CH_2Cl_2 was stirred under an H_2 atmosphere 25 °C for 12 h, filtered, and concentrated in vacuo to give 1.5 g (94%) of **24** as a white solid: ^{1}H NMR 7.82 (m, 2H), 7.74 (m, 2H), 7.68 (m, 2H), 7.32 (m, 2H), 6.58 (d, 2H, J = 14.5 Hz), 6.38 (s, 1H), 3.94 (d, 2H, J = 21.0 Hz), 3.77 (t, 2H, J = 7.0 Hz), 2.77 (m, 2H), 2.10 (m, 2H), ^{13}C NMR 177.5, 168.2, 163.9, 160.5, 159.7, 144.6, 133.8, 131.9, 129.0, 128.7, 128.2, 127.8, 125.9, 123.0, 109.0, 108.3, 96.0, 92.7, 56.3, 55.6, 37.5, 32.9, 29.1; HRMS $(M)^+$ (FAB) m/z (M + H) calcd for $C_{28}H_{23}O_6N$ 469.1525, found 469.1513.

5,7-Dimethoxy-4′-(3-aminoprop-1-yl)flavone (28). A mixture of 5,7-dimethoxy-4′-[3-(*N*-phthalimido)prop-1-yl]flavone (**24**) (120 mg, 0.26 mmol) in 20 mL of CH_2Cl_2 containing 1 mL N_2H_4−H_2O at 25 °C was stirred for 12 h and concentrated in vacuo. An aqueous solution of the residue was extracted with CH_2Cl_2, acidified to pH 3.0 by the addition of 1 M HCl, and extracted with CH_2Cl_2. The aqueous layer was made alkaline by addition of 1 M NaOH and extracted with CH_2Cl_2. The CH_2Cl_2 extracts were concentrated in vacuo to give 65 mg (73%) of 5,7-dimethoxy-4′-[3-aminoprop-1-yl]flavone (**28**) as a yellow solid: ^{1}H NMR 7.78 (d, 2H, J = 7.9 Hz), 7.31 (d, 2H, J = 7.9 Hz), 6.63 (s, 1H), 6.56 (s, 1H), 6.48 (s, 1H), 6.38 (s, 1H), 3.91 (m 2H), 2.71 (m, 4H), 1.78 (m, 2H); ^{13}C NMR 177.6, 163.9, 160.9, 160.8, 159.9, 145.9, 129.1, 129.0, 128.0, 126.0, 109.3, 108.6, 96.1, 92.8, 56.4, 55.7, 41.6, 35.1, 33.2; HRMS (FAB) m/z $(M)^+$ calcd for $C_{20}H_{22}O_4N$ 340.1760, found 340.1751.

5,7-Dihydroxy-4′-(3-aminoprop-1-yl)flavone (7). A slurry of 5,7-dimethoxy-4′-(3-aminoprop-1-yl)flavone (**28**) (65 mg, 0.19 mmol) and BBr_3 (2.0 mL of 1.0 M in CH_2Cl_2, 2.00 mmol) in 10 mL of dry $CHCl_3$ was stirred at reflux for 12 h, cooled to 25 °C, quenched by addition of MeOH, and concentrated in vacuo. The residue was partitioned between CH_2Cl_2 and 1 M NaOH. The aqueous layer was washed with CH_2Cl_2, acidified to pH 7 with 1 M

dx.doi.org/10.1021/jo3018473 | J. Org. Chem. 2013, 78, 1910−1922

HCl, and concentrated in vacuo to give a residue, which was dissolved in MeOH containing a large excess of *n*-butylamine. The resulting mixture was stirred at 25 °C for 12 h and concentrated in vacuo giving a residue, which was subjected to HPLC separation (C_{18} reversed-phase, H_2O−MeOH gradient). Concentration of combined fractions in vacuo afforded 13 mg (21%) of 5,7-dihydroxy-4′-(3-aminoprop-1-yl)flavone (**7**) as a yellow solid: ^{1}H NMR 7.91 (d, 2H, *J* = 8.3 Hz), 7.42 (d, 2H, *J* = 8.3 Hz), 6.67 (s, 1H), 6.45 (d, 1H, J= 7.0 Hz), 6.21 (d, 1H, *J* = 7 Hz), 2.97 (m, 2H), 2.81 (m, 2H), 2.02 (m, 2H); ^{13}C NMR 183.8, 166.5, 165.5, 163.2, 159.5, 146.4, 130.7, 130.3, 127.7, 105.7, 105.5, 100.3, 95.2, 40.3, 33.3, 30.0; HRMS (FAB) *m*/*z* (M + H)$^+$ calcd for $C_{18}H_{18}O_4N$ 312.1236, found 312.1246.

5,7-Dimethoxy-4′-[3-(*N*-phthalimido)but-1-en-1-yl]flavone (21). A mixture of 1.0 g (2.8 mmol) of 5,7-dimethoxy-4′-bromoflavone (**15**), 0.6 g (3.0 mmol) of 1-buten-4-ylphthalimide **17**, 100 mg (0.3 mmol) of P(*o*-tol)$_3$, and 500 mg (0.5 mmol) of $Pd_2(dba)_3$ in 50 mL of triethylamine was stirred at 110 °C for 12 h, cooled to 25 °C, and concentrated in vacuo. A solution of the residue in CH_2Cl_2 was washed with H_2O, dried, and concentrated in vacuo, giving a residue which was subjected to flash chromatography (silica gel, EtOAc−EtOH) to give 0.8 g (61%) of **21**: ^{1}H NMR 7.81 (m, 2H), 7.79 (m, 2H), 7.69 (m, 2H), 7.38 (m, 2H), 6.63 (m, 1H), 6.54 (m, 1H), 6.45 (m, 1H), 6.36 (s, 1H), 6.31 (m, 1H), 3.92 (d, 6H, *J* = 21 Hz), 3.70 (t, 2H, *J* = 7 Hz), 2.63 (m, 2H); ^{13}C NMR 177.5, 168.3, 164.0, 160.8, 160.3, 159.8, 140.0, 133.9, 132.0, 131.5, 130.0, 128.7, 126.5, 126.1, 123.2, 108.6, 96.1, 92.8, 56.4, 55.7, 37.3, 32.3; HRMS (FAB) *m*/*z* (M + H)$^+$ calcd for $C_{29}H_{24}O_6N$ 482.1604, found 482.1628.

5,7-Dimethoxy-4′-[3-(*N*-phthalimido)but-1-yl]flavone (25). A solution of 5,7-dimethoxy-4′-[3-(*N*-phthalimido)but-1-en-1-yl]flavone (**21**) (0.8 g, 1.7 mmol) and 10% Pd/C (0.1 g) in 40 mL of CH_2Cl_2 was stirred under 1 atm of H_2 at 25 °C and filtered. The filtrate was concentrated in vacuo to give **25** (0.7 g, 87%): ^{1}H NMR 7.81 (m, 2H), 7.75 (m, 2H), 7.68 (m, 2H), 7.27 (m, 2H), 6.3 (s, 1H), 6.53 (s, 1H), 6.35 (s,1H), 3.91 (d, 2H, *J* = 32 Hz), 3.70 (t, 2H, *J* = 6 Hz), 2.71 (t, 2H, *J* = 7.2 Hz), 1.71 (m, 4H); ^{13}C NMR 177.6, 168.2, 163.9, 160.7, 159.7, 145.6, 133.8, 131.9, 128.9, 125.9, 123.0, 108.3, 96.1, 92.7, 56.5, 55.6, 37.5, 35.6, 28.1, 27.9; HRMS (FAB) *m*/*z* (M + H)$^+$ calcd for $C_{29}H_{26}O_6N$ 484.1760, found 484.1776.

5,7-Dimethoxy-4′-(3-aminobut-1-yl)flavone (29). A solution of 5,7-dimethoxy-4′-[3-(*N*-phthalimido)but-1-yl]flavone (**25**) (700 mg, 1.45 mmol) and 1 mL of $NH_2NH_2{\cdot}H_2O$ in CH_2Cl_2 (20 mL) was stirred at 25 °C for 12 h and concentrated in vacuo. A CH_2Cl_2 solution of the residue was extracted with aqueous acid (pH 3.0). The aqueous solution was made basic and extracted with CH_2Cl_2. The CH_2Cl_2 extract was concentrated in vacuo to give **29** (450 mg, 88%): ^{1}H NMR 7.54 (d, 2H, *J* = 7.8 Hz), 7.0 (d, 2H, *J* = 7.8 Hz), 6.40 (s, 1H), 6.32 (s, 1H), 6.12 (s, 1H), 3.70 (d, 2H, *J* = 17 Hz), 2.53 (t, 2H, *J* = 6.7 Hz), 2.47 (t, 2H, *J* = 7.6 Hz), 1.49 (m, 2H), 1.31 (m, 2H); ^{13}C NMR 177.7, 163.9, 160.9, 159.9, 146.2, 129.0, 128.6, 127.5, 109.3, 108.5, 96.1, 92.8, 56.4, 55.7, 41.7, 35.6, 33.3, 28.4; HRMS (FAB) *m*/*z* (M + H)$^+$ calcd for $C_{21}H_{24}O_4N$ 354.1705, found 354.1696.

5,7-Dihydroxy-4′-(3-aminobut-1-yl)flavone (8). A mixture of 5,7-dimethoxy-4′-[3-aminobut-1-yl]flavone (**29**) (50 mg, 0.14 mmol) and BBr_3 (1 mL of 1.0 M in CH_2Cl_2, 1.00 mmol) in 10 mL of $CHCl_3$ was stirred at reflux for 12 h, cooled, diluted with MeOH, and concentrated in vacuo. The residue was partitioned between CH_2Cl_2 and 1 M NaOH. The aqueous layer was separated, washed with CH_2Cl_2, and acidified to pH 7 by addition of 1 M HCl. The solution was concentrated to give a residue, which was dissolved in MeOH and diluted by addition of butylamine. The mixture was stirred at 25 °C for 12 h and concentrated in vacuo giving a residue which was subjected to HPLC (ultrasphere C_{18} reversed-phase column and H_2O−MeOH) to afford 19 mg of **8** (31%): ^{1}H NMR (CD_3OD) 7.89 (d, 2H, *J* = 8 Hz), 7.40 (d, 2H, *J* = 8 Hz), 6.69 (s, 1H), 6.46 (s, 1H), 6.21 (s, 1H), 3.21 (m, 2H), 2.96 (m, 4H); 2.77 (m, 2H); ^{13}C NMR (CD_3OD) 183.9, 166.2, 165.7, 163.3, 159.5, 147.7, 130.4, 127.9, 105.5, 100.3, 95.1, 40.6, 36.0, 28.9, 28.1; HRMS (FAB) *m*/*z* (M + H)$^+$ calcd for $C_{19}H_{20}O_4N$ 326.1318, found 326.1379.

5,7-Dimethoxy-4′-[3-(*N*-phthalimido)pent-1-en-1-yl]flavone (22). A mixture of 3.0 g (8.3 mmol) of 5,7-dimethoxy-4′-bromoflavone (**15**), 1.9 g (8.8 mmol) of 1-buten-4-ylphthalimide **18**, 100 mg (0.3 mmol) of P(*o*-tol)$_3$, and 500 mg (0.5 mmol) of $Pd_2(dba)_3$ in 50 mL of triethylamine was stirred at 110 °C for 12 h, cooled to 25 °C, and concentrated in vacuo. A solution of the residue in CH_2Cl_2 was washed with H_2O, dried, and concentrated in vacuo, giving a residue which was subjected to flash chromatography (silica gel, EtOAc−EtOH) to give 2.1 g (51%) of **22**: ^{1}H NMR 7.75 (m, 2H), 7.67 (d, 2H, *J* = 8 Hz), 7.61 (m, 2H), 7.31 (d, 2H, *J* = 8 Hz), 6.60 (s, 1H), 6.47 (s, 1H), 6.37 (d, 1H, *J* = 16 Hz), 6.29 (s, 1H), 6.26 (m, 1H), 3.81 (d, 6H, *J* = 26), 3.69 (t, 2H, *J* = 7 Hz), 2.25 (q, 2H, *J* = 9 Hz), 1.85 (m, 2H); ^{13}C NMR 177.3, 168.2, 164.0, 160.5, 160.1, 159.5, 140.2, 133.7, 131.8, 131.5, 129.5, 129.4, 126.1, 125.8, 122.9, 108.2, 95.9, 92.6, 56.1, 55.5, 37.3, 30.2, 27.6; HRMS (FAB) *m*/*z*:(M + H)$^+$ calcd for $C_{30}H_{26}O_6N$ 496.1760, found 496.1745.

5,7-Dimethoxy-4′-[3-(*N*-phthalimido)pent-1-yl]flavone (26). A solution of 5,7-dimethoxy-4′-[3-(*N*-phthalimido)pent-1-en-1-yl]-flavone (**22**) (1.6 g,3.2 mmol) and 10% Pd/C (0.1 g) in 40 mL of CH_2Cl_2 was stirred under 1 atm of H_2 at 25 °C for 12 h and filtered. The filtrate was concentrated in vacuo to give **26** (1.2 g, 75%): ^{1}H NMR 7.80 (d, 2H, *J* = 2.85 Hz), 7.73 (m, 2H), 7.67 (d, 2H, *J* = 2.2 Hz), 7.25 (d, 2H, *J* = 9.5 Hz), 6.6 (s, 1H), 6.53 (s, 1H), 6.35 (s, 1H), 3.91 (d, 2H, *J* = 21.3 Hz), 3.66 (t, 2H, *J* = 2.1 Hz), 2.65 (t, 2H, *J* = 7.3 Hz), 1.66 (m, 6H); ^{13}C NMR 176.7, 167.5, 163.2, 159.9, 158.9, 145.4, 133.2, 131.2, 128.2, 128.0.126.8, 125.1, 122.3, 108.1, 107.3, 95.3, 92.1, 55.5, 55.1, 37.0, 34.7, 29.7, 27.5, 25.6 ; HRMS (FAB) *m*/*z* (M + H)$^+$ calcd for $C_{30}H_{28}O_6N$ 498.1917, found 498.1923.

5,7-Dimethoxy-4′-(3-aminopent-1-yl)flavone (30). A solution of 5,7-dimethoxy-4′-[3-(*N*-phthalimido)pent-1-yl]flavone (**26**) (900 mg, 1.45 mmol) and 1 mL of $NH_2NH_2{\cdot}H_2O$ in CH_2Cl_2 (20 mL) was stirred at 25 °C for 12 h and concentrated in vacuo. A CH_2Cl_2 solution of the residue was extracted with aqueous acid (pH 3.0). The aqueous solution was made basic and extracted with CH_2Cl_2. The CH_2Cl_2 extract was concentrated in vacuo to give **30** (526 mg, 79%): ^{1}H NMR 7.77 (m, 2H), 7.28 (m, 2H), 6.63 (s, 1H), 6.54 (d, 1H, *J* = 1.85 Hz), 6.35 (s, 1H), 3.91 (d, 2H, *J* = 18.8 Hz), 2.68 (m, 2H), 2.47 (t, 2H, *J* = 7.6 Hzd), 1.64 (m, 4H), 1.45 (m, 2H), 1.37 (m, 2H); ^{13}C NMR 177.4, 163.8, 160.6, 159.6, 146.2, 128.7, 127.4, 125.8, 125.7, 109.0, 108.1, 95.9, 92.6, 56.1, 55.5, 55.0, 41.8, 35.0, 32.8, 30.2, 26.3; HRMS (FAB) *m*/*z* (M + H)$^+$ calcd for $C_{22}H_{26}O_4N$ 368.1862, found 368.1847.

5,7-Dihydroxy-4′-(3-aminopent-1-yl)flavone (9). A mixture of 5,7-dimethoxy-4′-[3-aminopent-1-yl]flavone (**30**) (50 mg, 0.14 mmol) and BBr_3 (1 mL of 1.0 M in CH_2Cl_2, 1.00 mmol) in 10 mL of $CHCl_3$ was stirred at reflux for 12 h, cooled, diluted with MeOH, and concentrated in vacuo. The residue was partitioned between CH_2Cl_2 and 1 M NaOH. The aqueous layer was separated, washed with CH_2Cl_2, and acidified to pH 7 by addition of 1 M HCl. The solution was concentrated to give a residue, which was dissolved in MeOH and diluted by addition of butylamine. The mixture was stirred at 25 °C for 12 h and concentrated in vacuo giving a residue which was subjected to HPLC (ultrasphere C_{18} reversed-phase column and H_2O−MeOH) to afford 15 mg of **9** (32%): ^{1}H NMR (CD_3OD) 7.70 (d, 2H, *J* = 8.0 Hz), 7.40 (d, 2H, *J* = 8.0 Hz), 6.70 (s, 1H), 6.48 (s, 1H), 6.23 (s, 1H), 2.92 (t, 2H, *J* = 7.5 Hz), 2.75 (d, 2H, *J* = 7.5 Hz), 1.72 (m, 4H), 1.45(m, 2H); ^{13}C NMR (CD_3OD) 183.9, 166.2, 165.8, 163.3, 159.5, 148.3, 130.3, 127.6, 105.5, 100.3, 95.1, 40.7, 36.4, 31.7, 28.9, 27.0; HRMS (FAB) *m*/*z* (M + H)$^+$ calcd for $C_{20}H_{22}O_4N$ 340.1549, found 340.1562.

5,7-Dimethoxy-4′-[3-(*N*-phthalimido)hex-1-en-1-yl]flavone (23). A mixture of 1.6 g (4.4 mmol) of 5,7-dimethoxy-4′-bromoflavone (**14**), 1.2 g (5.2 mmol) of 1-buten-4-ylphthalimide **19**, 100 mg (0.3 mmol) of P(*o*-tol)$_3$, and 500 mg (0.5 mmol) of $Pd_2(dba)_3$ in 50 mL of triethylamine was stirred at 110 °C for 12 h, cooled to 25 °C, and concentrated in vacuo. A solution of the residue in CH_2Cl_2 was washed with H_2O, dried, and concentrated in vacuo, giving a residue which was subjected to flash chromatography (silica gel, EtOAc−EtOH) to give 1.2 g (51%) of **23**: ^{1}H NMR 7.81 (m, 2H), 7.76 (d, 2H, *J* = 8.4 Hz), 7.69 (m, 2H), 7.40 (d, 2H, *J* = 8.4 Hz), 6.63 (s, 1H), 6.54 (d, 1H, *J* = 2.1 Hz), 6.40 (d, 1H, *J* = 15.9 Hz), 6.35 (s, 1H), 6.33 (m, 1H), 3.91 (d, 6H, *J* = 20.9 Hz), 3.70 (t, 2H, *J* = 7.2 Hz), 2.28 (q, 2H, *J* = 7.2 Hz), 1.72 (m, 2H), 1.55(m, 2H); ^{13}C NMR 177.5, 168.3, 163.9,

dx.doi.org/10.1021/jo3018473 | J. Org. Chem. 2013, 78, 1910−1922

160.7, 160.4, 159.7, 140.5, 133.8, 132.6,132.0,129.5, 129.4, 126.3, 126.0, 125.8, 123.0, 109.1, 108.3, 96.0, 92.7, 56.3, 55.6, 37.6; 32.5, 28.0, 26.2; HRMS (FAB) m/z (M + Na)$^+$ calcd for $C_{33}H_{31}O_6NNa$ 538.2230, found 538.2243.

5,7-Dimethoxy-4′-[3-(*N*-phthalimido)hex-1-yl]flavone (27). A solution of 5,7-dimethoxy-4′-[3-(*N*-phthalimido)hex-1-en-1-yl]flavone (**23**) (1.0 g, 2.0 mmol) and 10% Pd/C (0.1 g) in 40 mL of CH_2Cl_2 was stirred under 1 atom of H_2 at 25 °C for 12 h and filtered. The filtrate was concentrated in vacuo to give **27** (1.2 g, 82%): ^{1}H NMR 7.70 (m, 4H), 7.73 (m, 2H), 7.25 (m, 2H), 6.65 (m, 1H), 6.59 (m, 1H), 6.36 (m, 1H), 3.92 (d, 2H, J = 20.3 Hz), 3.66 (t, 2H, J = 7.3 Hz), 2.64 (t, 2H, J = 7.7 Hz), 1.66 (m, 4H), 1.46 (m, 2H), 1.23(m,2H); ^{13}C NMR 177.1, 167.9, 163.6, 160.4, 160.2, 159.3, 146.0, 133.4, 131.5, 130.8, 128.5, 128.2, 127.8, 125.4, 122.6, 108.5, 108.2, 107.7, 95.7, 92.4, 55.9, 55.3, 37.4, 35.2, 30.4, 29.2, 28.0, 26.2; HRMS (FAB) m/z (M + H)$^+$ calcd for $C_{31}H_{31}O_6N$ 512.2073, found 512.2080.

5,7-Dimethoxy-4′-(3-aminohex-1-yl)flavone (31). A solution of 5,7-dimethoxy-4′-[3-(*N*-phthalimido)hex-1-yl]flavone (**27**) (800 mg, 1.6 mmol) and 1 mL of $NH_2NH_2{\cdot}H_2O$ in CH_2Cl_2 (20 mL) was stirred at 25 °C for 12 h and concentrated in vacuo. A CH_2Cl_2 solution of the residue was extracted with aqueous acid (pH 3.0). The aqueous solution was made basic and extracted with CH_2Cl_2. The CH_2Cl_2 extract was concentrated in vacuo to give **31** (428 mg, 72%): ^{1}H NMR 7.74 (d, 2H, J = 7.0 Hz), 7.25 (m, 2H), 6.62 (s, 1H), 6.54 (d, 1H, J = 1.0 Hz), 6.34 (s, 1H), 3.90 (d, 2H, J = 19.8 Hz), 2.63 (m, 4H), 1.67 (m, 2H), 1.52 (m, 2H), 1.33 (m, 4H); ^{13}C NMR 177.5, 163.9, 160.7, 159.7, 146.4, 128.8, 125.8, 109.1, 108.2, 96.0, 92.7, 56.2, 55.6, 41.4, 35.6, 32.2, 31.0, 28.9, 26.5; HRMS (FAB) m/z (M + H)$^+$ calcd for $C_{23}H_{28}O_4N$ 382.2018, found 382.2010.

5,7-Dihydroxy-4′-(3-aminohex-1-yl)flavone (10). A mixture of 5,7-dimethoxy-4′-(3-aminohex-1-yl)flavone (**31**) (50 mg, 0.13 mmol) and BBr_3 (1 mL of 1.0 M in CH_2Cl_2, 1.00 mmol) in 10 mL of $CHCl_3$ was stirred at reflux for 12 h, cooled, diluted with MeOH, and concentrated in vacuo. The residue was partitioned between CH_2Cl_2 and 1 M NaOH. The aqueous layer was separated, washed with CH_2Cl_2, and acidified to pH 7 by addition of 1 M HCl. The solution was concentrated to give a residue, which was dissolved in MeOH and diluted by addition of *n*-butylamine. The mixture was stirred at 25 °C for 12 h and concentrated in vacuo giving a residue which was subjected to HPLC (ultrasphere C_{18} reversed-phase column and H_2O−MeOH) to afford 15 mg of **10** (32%): ^{1}H NMR (CD_3OD) 7.70 (m, 2H), 7.39 (d, 2H, J = 7.9 Hz), 6.69 (s, 1H), 6.48 (s, 1H), 6.23 (s, 1H), 2.93 (t, 2H, J = 7.2 Hz), 2.73 (t, 2H, J = 7.5 Hz), 1.70 (m, 4H), 1.33(m, 2H), 1.00(m, 2H); ^{13}C NMR (CD_3OD) 183.8, 166.1, 165.7, 163.2, 159.4, 148.6, 130.3, 129.9, 127.4, 105.5, 105.4, 100.3, 95.1, 40.7, 36.6, 31.9, 29.7, 28.5, 27.3.

5,7-Dimethoxy-4′-(3-aminobut-1-en-1-yl)flavone (32). A solution of 5,7-dimethoxy-4′-[3-(*N*-phthalimido)but-1-en-1-yl]flavone (**21**) (300 mg, 0.62 mmol) and 1 mL of $NH_2NH_2{\cdot}H_2O$ in CH_2Cl_2 (20 mL) was stirred at 25 °C for 12 h and concentrated in vacuo. A CH_2Cl_2 solution of the residue was extracted with aqueous acid (pH 3.0). The aqueous solution was made basic and extracted with CH_2Cl_2. The CH_2Cl_2 extract was concentrated in vacuo to give **32** (162 mg, 74%): ^{1}H NMR 7.78 (d, 2H, J = 7.8 Hz), 7.44 (d, 2H, J =7.8 Hz), 6.64(s, 1H), 6.65 (s, 1H), 6.48 (d, 1H, J = 15.8 Hz), 6.36 (s, 1H), 6.32 (m, 1H), 3.92 (d, 2H, J = 20.2 Hz), 2.86 (t, 2H, J= 6.0 Hz), 2.39 (m, 2H); ^{13}C NMR 177.6, 164.0, 161.0,160.3, 159.8, 140.3, 129.8, 129.0, 126.4, 126.1, 109.3, 108.6, 96.1, 92.8, 56.4, 55.7, 41.5, 37.4; HRMS (FAB) m/z (M + H)$^+$ calcd for $C_{21}H_{22}O_4N$ 352.1549, found 352.1559.

5,7-Dihydroxy-4′-(3-aminobut-1-en-1-yl)flavone (12). A mixture of 5,7-dimethoxy-4′-(3-aminobut-1-en-1-yl)flavone (**32**) (100 mg, 0.28 mmol) and BBr_3 (1 mL of 1.0 M in CH_2Cl_2, 1.00 mmol) in 10 mL of $CHCl_3$ was stirred at reflux for 12 h, cooled, diluted with MeOH, and concentrated in vacuo. The residue was partitioned between CH_2Cl_2 and 1 M NaOH. The aqueous layer was separated, washed with CH_2Cl_2, and acidified to pH 7 by addition of 1 M HCl. The solution was concentrated to give a residue, which was dissolved in MeOH and diluted by addition of butylamine. The mixture was stirred at 25 °C for 12 h and concentrated in vacuo giving a residue which was subjected to HPLC (ultrasphere C_{18} reversed-phase column and H_2O−MeOH) to afford 28 mg of **12** (31%): ^{1}H NMR (CD_3OD) 7.89 (d, 2H, J = 37.8 Hz), 7.55 (d, 2H, J = 22.5 Hz), 6.61 (m, 2H), 6.42 (m, 2H), 6.18 (s, 1H), 2.91 (t, 2H, J = 7.3 Hz), 2.63 (m, 2H); ^{13}C NMR (CD_3OD) 183.7, 166.2, 165.1, 163.2, 159.4, 142.0, 133.8, 131.2, 128.4, 128.0, 127.6, 105.7, 105.6, 100.3, 95.1, 40.2, 32.1; HRMS (FAB) m/z (M + H)$^+$ calcd for $C_{19}H_{18}O_4N$ 324.1236, found 324.1208.

Synthesis of Aminoalkylflavone 11 (Scheme 3). 5,7-Dimethoxy-3′-bromoflavone (34). To a solution of methyl 3-bromobenzoate (**33**) (9.80 g, 45.5 mmol) and NaH 1.20 g (95% dispersion, 50 mmol) in DMF (20 mL) at 0 °C was added a solution of 2,4-dimethoxy-6-hydroxyacetophenone **13** (3.00 g, 15.2 mmol) in DMF (50 mL). The mixture was stirred at 25 °C for 12 h and poured onto ice. The pH of the resulting solution was adjusted to 10 by addition of 1 N HCl and extracted with CH_2Cl_2. The CH_2Cl_2 extracts were concentrated in vacuo giving a residue, which was dissolved in $CHCl_3$. The $CHCl_3$ solution was saturated with gaseous HCl, stirred for 4 h at 25 °C, made basic by the addition of aq Na_2CO_3, and extracted with CH_2Cl_2. The CH_2Cl_2 extracts were dried and concentrated in vacuo giving a solid which was crystallized from DMF to afford 2.28 g (42%) of 3,5-dimethoxy-3′-bromoflavone (**34**) as white solid: ^{1}H NMR 7.99 (s, 1H), 7.73 (d, 2H, J = 7.8 Hz), 7.59 (d, 1H, J = 7.95 Hz), 7.35 (m, 1H), 6.62 (s, 1H), 6.55 (d, 1H, J = 1.9 Hz), 6.35 (d, 1H, J = 1.7 Hz), 3.91 (d, 2H, J = 15.0 Hz); ^{13}C NMR 176.0, 163.3, 163.0, 159.8, 158.7, 157.7,133.1, 132.4, 129.7128.1, 127.7, 124.9, 123.5, 122.2, 108.4,108.1, 95.5, 92.0, 55.5, 55.1; HRMS (FAB) m/z (M)$^+$ calcd for $C_{17}H_{13}O_4{}^{79}Br$ 361.0075, found 361.0073.

5,7-Dimethoxy-3′-[3-(*N*-phthalimido)hex-1-yl]flavone (35). A mixture of 1.6 g (4.4 mmol) of 5,7-dimethoxy-4′-bromoflavone (**34**), 1.2 g (5.2 mmol) of 1-hexen-4-ylphthalimide (**19**), 100 mg (0.3 mmol) of P(*o*-tol)$_3$, and 500 mg (0.5 mmol) of $Pd_2(dba)_3$ in 50 mL of triethylamine was stirred at 110 °C for 12 h, cooled to at 25 °C, and concentrated in vacuo. A solution of the residue in CH_2Cl_2 was washed with H_2O, dried, and concentrated in vacuo. The residue containing of crude 5,7-dimethoxy-3′-[3-(*N*-phthalimido)hex-1-en-1-yl]flavone was used for the next step without purification. A 40 mL volume of CH_2Cl_2 was added to the above residue followed by adding 10% Pd/C (0.1 g). The mixture was stirred under 1 atom of H_2 at 25 °C for 12 h and filtered. The filtrate was concentrated in vacuo. The residue was subjected to flash chromatography (silica gel, EtOAc−EtOH) to give **35** (1.2 g, 53%): ^{1}H NMR 7.80 (m, 2H), 7.67 (m, 2H), 7.48 (m, 1H), 7.36(m, 1H), 7.28 (m, 1H), 6.65 (m, 1H), 6.57 (s, 1H), 6.35 (s, 1H), 3.91 (d, 2H, J = 17.7 Hz), 3.67 (tm, 4H), 2.64 (m, 2H), 1.65 (m, 4H), 1.38 (m, 2H); ^{13}C NMR 177.6, 168.4, 164.0, 160.9, 160.0, 143.5, 133.8, 132.1,131.5, 130.8, 128.9, 128.8, 125.9, 123.7, 109.0, 96.2, 92.9, 56.4, 55.8, 37.9, 35.8, 31.1, 28.7, 28.4, 26.6.

5,7-Dihydroxy-3′-(3-aminohex-1-yl)flavone (11). A solution of 5,7-dimethoxy-4′-[3-(*N*-phthalimido)hex-1-yl]flavone (**35**) (500 mg, 0.98 mmol) and 1 mL of $NH_2NH_2{\cdot}H_2O$ in CH_2Cl_2 (20 mL) was stirred at 25 °C for 12 h and concentrated in vacuo. A CH_2Cl_2 solution of the residue was extracted with aqueous acid (pH 3.0). The aqueous solution was made basic and extracted with CH_2Cl_2. The CH_2Cl_2 extract was concentrated in vacuo giving residue containing crude 5,7-dimethoxy-3′-(3-aminohex-1-yl)flavone, which was used for the next step without purification. A mixture of the above crude and BBr_3 (1 mL of 1.0 M in CH_2Cl_2, 1.00 mmol) in 10 mL of $CHCl_3$ was stirred at reflux for 12 h, cooled, diluted with MeOH, and concentrated in vacuo. The residue was partitioned between CH_2Cl_2 and 1 M NaOH. The aqueous layer was separated, washed with CH_2Cl_2, and acidified to pH 7 by addition of 1 M HCl. The solution was concentrated to give a residue, which was dissolved in MeOH and diluted by addition of n-butylamine. The mixture was stirred at 25 °C for 12 h and concentrated in vacuo giving a residue which was subjected to HPLC (ultrasphere C_{18} reversed-phase column and H_2O−MeOH) to afford 58 mg of **11** (17%): ^{1}H NMR (CD_3OD) 7.95 (m, 1H), 7.86 (m,1H), 7.62 (m, 1H), 7.44 (m, 1H) ; 6.76 (d, 1H, J = 12.2 Hz), 6.21 (s, 1H), 6.26 (s, 1H), 2.99 (t, 2H, J = 7.5 Hz), 2.92 (t, 2H, J = 7.9 Hz), 2.77 (t, 2H, J = 7.4 Hz), 2.36 (m, 2H), 1.75 (m, 2H), 1.65 (m, 2H); ^{13}C NMR (CD_3OD) 183.9, 166.3, 163.3, 159.6, 133.3, 130.3, 127.3, 125.0, 105.5,

dx.doi.org/10.1021/jo3018473 | J. Org. Chem. 2013, 78, 1910−1922

106.0, 100.3, 95.2, 40.7, 36.6, 32.3, 29.7, 28.5, 27.3; HRMS (FAB) m/z $(M + H)^+$ calcd for $C_{21}H_{24}O_4N$ 354.1705, found 354.1713.

Synthesis of (*E*)-3[4-(Morpholin-4-yl)benzylidenyl]indoline. To a solution of 7.5 mL of dimethylformamide in 25 mL of anhydrous 1,2-dichloroethane was added dropwise 5 mL (50 mmol) of phosphorus oxychloride at 0 °C. The mixture was stirred for 30 min at room temperature and cooled to 0 °C. 4-Phenylmorpholine (8.3 g, 51 mmol) was added portionwise over 15 min, and the mixture was stirred at reflux for 48 h. Then 1.25 mL of triethylamine was added, and the solution was stirred for another 24 h and poured into ice-cold 1 N sodium hydroxide solution. The pH was adjusted to 10, and the resulting mixture was stirred at room temperature for 1 h. The organic layer was separated and extracted with dichloromethane. The combined organic layer was washed with NaCl solution until pH = 7, dried over anhydrous sodium sulfate, and concentrated in vacuo giving a residue that was subjected to silica gel column chromatography, eluting with a mixture of ethyl acetate and hexane, to afford 5.6 g (58%) of 4-(morpholin-4-yl)benzaldehyde as a white solid: ^{1}H NMR (500 MHz, CDCl) 9.74 (s, 1H), 7.72 (m, 2H), 6.86 (m, 2H), 3.80 (m, 4H), 3.29 (t, 4H, J = 4.0 Hz) ppm. The spectroscopic data match those reported by Sun et al.[50]

A mixture of 2 g (15 mmol) of oxindole, 3 g (15 mmol) of 4-(morpholin-4-yl)benzaldehyde, and 2 mL of piperidine in 10 mL of ethanol was stirred at 90 °C for 24 h. The precipitate formed on cooling was separated by filtration, washed with cold ethanol, and dried to yield 3.1 g (68%) of (*E*)-3[4-(morpholin-4-yl)benzylidenyl]-indoline as a yellow solid: ^{1}H NMR (250 MHz, DMSO) 10.50 (s, 1H), 7.73 (d,1H, J = 7.9 Hz), 7.63 (d, 2H, J = 8.6 Hz), 7.53 (s, 1H), 7.18 (t, 1H, J = 7.6 Hz), 7.02 (d, 2H, J = 8.8 Hz), 6.87 (t, 2H, J = 7.4 Hz), 3.72 (t, 4H, J = 5.0 Hz), 3.24 (t, 4H, J = 4.7) ppm. The spectroscopic data match those reported in Sun et al.[50]

Flavone and Quercetin-3,5,7,3′,4′-pentamethyl Ether. Flavone and quercetin-3,5,7,3′,4′-pentamethyl ether were prepared by using the procedures described by Kim et al.[51] and Picq et al.,[52] respectively.

■ ASSOCIATED CONTENT

Supporting Information

Inhibition constants for pyruvate phosphate dikinase and ^{1}H and ^{13}C NMR spectra. This material is available free of charge via the Internet at http://pubs.acs.org.

■ AUTHOR INFORMATION

Corresponding Author

* Tel: 505-277-6390. Fax: 505-277-6202. E-mail: mariano@unm.edu.

Notes

The authors declare no competing financial interest.

■ ACKNOWLEDGMENTS

Financial support for these studies was provided by a grant from the NIH (GM36260). This contribution, as well as all others made by P.S.M. in the past, have benefited from the excellent and broad educational background that he received as a student in the late Professor Howard E. Zimmerman's laboratory at the University of Wisconsin—Madison. As a result, this contribution is dedicated to the memory of H.E.Z. and his numerous ground-breaking studies that helped create the foundation of the science of organic chemistry.

■ REFERENCES

(1) Wood, H. G.; O'Brien, W, E.; Micheales, G. *Adv. Enzymol. Relat. Areas Mol. Biol.* **1977**, *45*, 85−155.
(2) Michaels, G.; Milner, Y.; Moskovitz, B. R.; Wood, H. G. *J. Biol. Chem.* **1978**, *253*, 7656−7661.
(3) Moskovitz, B. R.; Wood, H. G. *J. Biol. Chem.* **1978**, *253*, 884−888.
(4) Wang, H. C.; Ciskanik, L.; Dunaway-Mariano, D. *Biochemistry* **1988**, *27*, 625−633.
(5) Thrall, H.; Mehl, A. F.; Carroll, L. J.; Dunaway-Mariano, D. *Biochemistry* **1993**, *32*, 1803−1809.
(6) Goss, N. H.; Evans, C. T.; Wood, H. G. *Biochemistry* **1980**, *19* (25), 5805−5809.
(7) Dunaway-Mariano, D. *Methods Enzymol.* **1999**, *308*, 149−176.
(8) Carroll, L. J.; Xu, Y.; Thrall, S. H.; Martin, B. M.; Dunaway-Mariano, D. *Biochemistry* **1994**, *33*, 1134−1142.
(9) Xu, Y.; McGuire, M.; Martin, B. M.; Dunaway-Mariano, D. *Biochemistry* **1995**, *34*, 2195−2202.
(10) Thrall, S. A.; Dunaway-Mariano, D. *Biochemistry* **1994**, *33*, 1103−1107.
(11) Herzberg, O.; Chen, C. C. H.; Kapadia, G.; McGuire, M.; Carroll, L. J.; Noh, S. J.; Dunaway-Mariano, D. *Proc. Natl. Acad. Sci. U.S.A.* **1996**, *93*, 2652−2657.
(12) Galperin, M. Y.; Koonin, E. V. *Protein Sci.* **1997**, *6* (12), 2639−2643.
(13) Lim, K.; Read, R. J.; Chen, C. C.; Tempczyk, A.; Wei, M.; Ye, D.; Wu, C.; Dunaway-Mariano, D.; Herzberg, O. *Biochemistry* **2007**, *46*, 14845−14853.
(14) Hatch, M. D.; Slack, C. R. *Biochem. J.* **1969**, *112*, 549−558.
(15) Hrdy, I.; Mertens, E.; Nohynkova, E. *Exp. Parasitol.* **1993**, *76*, 438−441.
(16) Raverdy, S.; Foster, J. M.; Roopenian, E.; Carlow, C. K. *Mol. Biochem. Parasitol.* **2008**, *160*, 163−166.
(17) Slamovits, C. H.; Keeling, P. J. *Eukaryotic Cell* **2006**, *5*, 148−154.
(18) Bringaud, F.; Baltz, D.; Baltz, T. *Proc. Natl. Acad. Sci. U.S.A.* **1998**, *95*, 7963−7968.
(19) Benziman, M.; Eizen, N. *J. Biol. Chem.* **1971**, *246*, 57−61.
(20) Reeves, R. E.; Menzies, R. A.; Hsu, D. S. *J. Biol. Chem.* **1968**, *243*, 5486−5491.
(21) Marshall, J. S.; Ashton, A. R.; Govers, F.; Hardham, A. R. *Current Genetics* **2001**, *40*, 73−81.
(22) Liapounova, N. A.; Hampl, V.; Gordon, P. M.; K., Sensen, C. W.; Gedamu, L.; Dacks, J. B. *Eukaryotic Cell* **2006**, *5*, 2138−2146.
(23) Coustou, V.; Besterio, S.; Biran, M.; Diolez, P.; Bouchaud, V.; Voisin, P.; Michels, P. A. M.; Canion, P; Baltz, T.; Bringaud, F. *J. Biol. Chem.* **2003**, *278*, 49625−49635.
(24) Crafts-Brandner, S. J.; Salvucci, M. E. *Plant Physiol.* **2002**, *129* (4), 1773−1780.
(25) Eisen, J. A.; Nelson, K. E.; Paulsen, I. T.; Heidelberg, J. F.; Wu, M.; Dodson, R. J.; Deboy, R.; Gwinn, M. L.; Nelson, W. C.; Haft, D. H.; Hickey, E. K.; Peterson, J. D.; Durkin, A. S.; Kolonay, J. L.; Yang, F.; Holt, I.; Umayam, L. A.; Mason, T.; Brenner, M.; Shea, T. P.; Parksey, D.; Nierman, W. C.; Feldblyum, T. V.; Hansen, C. L.; Craven, M. B.; Radune, D.; Vamathevan, J.; Khouri, H.; White, O.; Gruber, T. M.; Ketchum, K. A.; Venter, J. C.; Tettelin, H.; Bryant, D. A.; Fraser, C. M. *Proc. Natl. Acad. Sci. U.S.A.* **2002**, *99* (14), 9509−9514.
(26) Acosta, H.; Dubourdieu, M.; Quinones, W. A.; Caceres, A.; Bringaud, F.; Concepcion, J. L. *Comp. Biochem. Physiol. B Bichem Mol. Biol.* **2004**, *138*, 347−356.
(27) Saavedra, E.; Encalada, R.; Pineda, E.; Jasso-Chavez, R.; Moreno-Sanchez, R. *FEBS J.* **2005**, *272*, 1767−1783.
(28) Feng, X. M.; Cao, L. J.; Adam, R. D.; Zhang, X. C.; Lu, S. Q. *Biochem. Biophys. Res. Commun.* **2008**, *367*, 394−398.
(29) Lawyer, A. L.; Kelley, S. R.; Allen, J. I. *Z. Naturforsch., C: Biosci.* **1987**, *42* (6), 834−836.
(30) Norman, R. A.; Toader, D.; Feruson, D. *Trends Pharmacol. Sci.* **2012**, *33*, 273−278.
(31) Fawaz, M. V.; Topper, M. E.; Firestine, S. M. *Bioorg. Chem.* **2011**, *39*, 185−191.
(32) Mochalkin, I.; Miller, J. R.; Narasimhan, L.; Thanabal, V.; Erdman, P.; Cox, P. B.; Prasad, J. V. N. V.; Lightle, S.; Huband, M. D.; Stover, C. K. *ACS Chem. Biol.* **2009**, *6*, 473−483.

(33) SaavedraLira, E.; PerezMontfort, R. *Arch. Med. Res.* **1996**, *27*, 257−264.
(34) Haines, D. S.; Burnell, J. N.; Doyle, J. R.; Llewellyn, L. E.; Motti, C. A.; Tapiolas, D. M. *J. Agric. Food Chem.* **2005**, *53*, 3856−3862.
(35) Motti, C. A.; Bourguet-Kondracki, M. L.; Longeon, A.; Doyle, J. R.; Llewellyn, L, E.; Tapiolas, D. M.; Yin, P. *Molecules* **2007**, *12*, 1376−1388.
(36) Motti, C. A.; Bourne, D. G.; Burnell, J. N.; Doyle, J. R.; Haines, D. S.; Liptrot, C. H.; Llewellyn, L. E.; Ludke, S.; Muirhead, A.; Tapiolas, D. M. *Appl. Environ. Microbiol.* **2007**, *73*, 1921−1927.
(37) Stephen, P.; Vijayan, R.; Bhat, A.; Subbarao, N.; Bamezai, R. N. *J. Comput. Aided Mol. Des.* **2008**, *22*, 647−660.
(38) Cosenza, L. W.; Bringaud, F.; Baltz, T.; Vellieux, F. M. D. *J. Mol. Biol.* **2001**, *318*, 1417−1432.
(39) Sielecki, T. M.; Boylan, J. F.; Benfield, P. A.; Trainor, G. L. *J. Med. Chem.* **2000**, *43* (1), 1−18.
(40) Bridges, A. J. *Chem. Rev.* **2001**, *101* (8), 2541−2571.
(41) Dumas, J. *Expert Opin. Ther. Pat.* **2001**, *11* (3), 405−429.
(42) Narayana, N.; Diller, T. C.; Koide, K.; Bunnage, M. E.; Nicolaou, K. C.; Brunton, L. L.; Xuong, N. H.; TenEyck, L. F.; Taylor, S. S. *Biochemistry* **1999**, *38* (8), 2367−2376.
(43) Norman, B. H.; Shih, C.; Toth, J. E.; Ray, J. E.; Dodge, J. A.; Johnson, D. W.; Rutherford, P. G.; Schultz, R. M.; Worzalla, J. F.; Vlahos, C. *J. Med. Chem.* **1996**, *39* (5), 1106−1111. Walker, E. H.; Pacold, M. E.; Perisic, O.; Stephens, L.; Hawkins, P. T.; Wymann, M. P.; Williams, R. L. *Mol. Cell* **2000**, *6* (4), 909−919.
(44) Baumgrass, R.; Weiwad, M.; Erdmann, F.; Liu, J. O.; Wunderlich, D.; Grabley, S.; Fischer, G. *J. Biol. Chem.* **2001**, *276* (51), 47914−47921.
(45) Pocalyko, D. J.; Carroll, L. J.; Martin, B. M.; Babbitt, P. C.; Dunaway-Mariano, D *Biochemistry* **1990**, *29*, 10757.
(46) Cleland, W. W. *Methods Enzymol.* **1979**, *63*, 103−138. Cleland, W. W. *Methods Enzymol.* **1979**, *63*, 500−513.
(47) Wei, M.; Li, Z.; Ye, D.; Herzberg, O.; Dunaway-Mariano, D. *J. Biol. Chem.* **2000**, *275*, 41156−41165.
(48) Zembower, D. E.; Zhang, H. *J. Org. Chem.* **1998**, *63*, 9300−9305.
(49) Delugo, G.; Faedda, G.; Gladiali, S. *J. Organomet. Chem.* **1984**, *268*, 167−174.
(50) Sun, L.; Tran, N.; Tang, F.; App, H.; Hirth, P.; McMahon, G.; Tang, C. *J. Med. Chem.* **1998**, *41* (14), 2588−2603.
(51) Kim, K. S. PCT Int. Appl. WO 9813344 A1 19980402, 1998; CAN 128:270537, AN 208527 5,908, 934.
(52) Picq, M.; Prigent, A. F.; Chabannes, B.; Pacheco, H. *Tetrahedron Lett.* **1984**, *25* (21), 2227−2230.